Phenylthiyl Radical Complexes of Gallium(III), Iron(III), and Cobalt(III) and Comparison with Their Phenoxyl Analogues

Shuji Kimura, Eckhard Bill, Eberhard Bothe, Thomas Weyhermüller, and Karl Wieghardt*

Contribution from the Max-Planck-Institut für Strahlenchemie, D-45470 Mülheim an der Ruhr, Germany

Received December 20, 2000

Abstract: Three hexadentate, asymmetric pendent arm macrocycles containing a 1,4,7-triazacyclononane-1,4-diacetate backbone and a third, *N*-bound phenolate or thiophenolate arm have been synthesized. In $[L^1]^{3-}$ the third arm is 3,5-di-*tert*-butyl-2-hydroxybenzyl, in $[L^2]^{3-}$ it is 2-mercaptobenzyl, and in $[L^3]^{3-}$ it is 3,5-di-*tert*-butyl-2-mercaptobenzyl. With trivalent metal ions these ligands form very stable neutral mononuclear complexes $[M^{III}L^1]$ (M = Ga, Fe, Co), $[M^{III}L^2]$ (M = Ga, Fe, Co), and $[M^{III}L^3]$ (M = Ga, Co) where the gallium and cobalt complexes possess an $S = 0$ and the iron complexes an $S = {}^5/_2$ ground state. Complexes $[CoL^1]\cdot CH_3OH\cdot 1.5H_2O$, $[CoL^3]\cdot 1.17H_2O$, $[FeL^1]\cdot H_2O$, and $[FeL^2]$ have been characterized by X-ray crystallography. Cyclic voltammetry shows that all three $[M^{III}L^1]$ complexes undergo a reversible, ligand-based, one-electron oxidation generating the monocations $[M^{III}L^{1\bullet}]^+$ which contain a coordinated phenoxyl radical as was unambiguously established by their electronic absorption, EPR, and Mössbauer spectra. In contrast, $[M^{III}L^2]$ complexes in CH_3CN solution undergo an irreversible one-electron oxidation where the putative thiyl radical monocationic intermediates dimerize with S−S bond formation yielding dinuclear disulfide species $[M^{III}L^2{-}L^2M^{III}]^{2+}$. $[GaL^3]$ behaves similarly despite the steric bulk of two tertiary butyl groups at the 3,5-positions of the thiophenolate, but $[Co^{III}L^3]$ in CH_2Cl_2 at −20 to −61 °C displays a reversible one-electron oxidation yielding a relatively stable monocation $[Co^{III}L^{3\bullet}]^+$. Its electronic spectrum displays intense transitions in the visible at 509 nm ($\epsilon = 2.6 \times 10^3$ M^{-1} cm^{-1}) and 670sh, 784 (1.03×10^3) typical of a phenylthiyl radical. The EPR spectrum of this species at 90 K proves the thiyl radical to be coordinated to a diamagnetic cobalt(III) ion ($g_{iso} = 2.0226$; $A_{iso}(^{59}Co) = 10.7$ G).

Introduction

Recently Stubbe et al.[1] have reported the observation of a kinetically competent thiyl radical intermediate in the ribonucleoside triphosphate reductase (RTPR) from *Lactobacillus leichmannii* by using rapid freeze quench techniques and EPR spectroscopy. From similarities in mechanism between RTPR and *Escherichia coli* ribonucleotide reductase (RNR) they proposed that the latter enzyme also requires a thiyl radical for catalysis. This radical is suggested to be a cysteinyl radical generated from C^{408} in RTPR and C^{439} in RNR.[1,2] In these enzymes the cysteinyl radical is not S-coordinated to a transition metal ion.

In contrast, in cytochrome P450[3] a high-valent iron−oxene species has been proposed as an intermediate in the catalytic cycle the electronic structure of which is currently discussed controversially. It may involve a porphyrin cation radical as is established for compound I in horseradish peroxidase[4] and some synthetic models,[5] or, alternatively an *S-coordinated* cysteinyl radical or a resonance hybrid of these forms. The spin state of the iron ion is also a matter of discussion. Lacking spectroscopic data a theoretical DFT study has recently been published.[6] The chemistry and spectroscopy of the phenylthiyl radical has been investigated in detail. The electronic spectrum,[7] the EPR[8] and resonance Raman spectrum[7] have been recorded and its structure has been deduced from ab initio calculations.[7] These data show that the C−S bond is essentially a single bond with the unpaired electron localized on the sulfur atom (Chart 1). This is in distinct contrast to the corresponding phenoxyl and anilino radical both of which show quinoide character with substantial delocalization of the unpaired electron over the respective phenyl ring.[9]

The unsubstituted phenylthiyl is extremely reactive; it decays via second-order kinetics with head-to-head dimerization ($2k = 9.6 \times 10^9$ M^{-1} s^{-1}), generating the disulfide Ph-S−S−Ph.[7] Even the sterically protected 2,4,6-*tert*-butylphenylthiyl decays within minutes,[10] whereas the corresponding phenoxyl and anilino radicals[11] are stable in CCl_4 solution for days.

While the coordination chemistry of (phenoxyl)metal complexes and their (anilino)metal analogues has in recent years

(1) Licht, S.; Gerfen, G. J.; Stubbe, J. *Science* **1996**, *271*, 477.
(2) Booker, S.; Licht, S.; Broderick, J.; Stubbe, J. *Biochemistry* **1994**, *33*, 12676.
(3) (a) Groves, J.; Hang, Y.-Z. In *Cytochrome P450: Structure Mechanisms and Biochemistry*, 2nd ed.; Ortiz-de Montellano, P. R., Ed.; Plenum: New York, 1995. (b) Woggon, W.-D. *Top. Curr. Chem.* **1996**, *184*, 40. (c) Sono, M.; Roach, M. P.; Coulter, E. D.; Dawson, J. H. *Chem. Rev.* **1996**, *96*, 2841.
(4) Schulz, C. E.; Rutter, R.; Sage, J. T.; Debrunner, P. G.; Hager, L. P. *Biochemistry* **1984**, *23*, 4743.
(5) Bill, E.; Ding, X.-Q.; Trautwein, A. X.; Winkler, H.; Mandon, D.; Weiss, R.; Gold, A.; Jayaraj, K.; Hatfield, W. E.; Kirk, M. L. *Eur. J. Biochem.* **1990**, *188*, 665.
(6) (a) Ogliaro, F.; Cohen, S.; Filatov, M.; Harris, N.; Shaik, S. *Angew. Chem.* **2000**, *112*, 4009; *Angew. Chem., Int. Ed.* **2000**, *39*, 3851. (b) Harris, N.; Cohen, S.; Filatov, M.; Ogliaro, F.; Shaik, S. *Angew. Chem.* **2000**, *112*, 2070; *Angew. Chem., Int. Ed.* **2000**, *39*, 2003.
(7) Tripathi, G. N. R.; Sun, Q.; Armstrong, D. A.; Chipman, D. M.; Schuler, R. H. *J. Phys. Chem.* **1992**, *96*, 5344.
(8) (a) Zandstra, P. J.; Michaelsen, J. D. *J. Chem. Phys.* **1963**, *39*, 933. (b) Schmidt, V. *Angew. Chem., Int. Ed. Engl.* **1964**, *3*, 602.
(9) Adamo, C.; Subra, R.; Di Matteo, A.; Barone, V. *J. Chem. Phys.* **1998**, *109*, 10244.

10.1021/ja004305p CCC: $20.00
Published on Web 06/02/2001

Chart 1

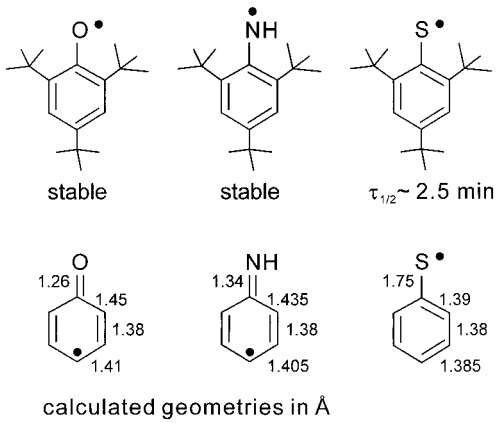

been well established,[12] this appears not to be the case for (thiyl)-metal complexes. The report by Darensbourg, Krusic, Amatore, et al.[13] describes the one-electron oxidation chemistry of $RS[Cr(CO)_5]_2^-$ —a diamagnetic 18e species—to the corresponding neutral radical species $R\dot{S}[Cr(CO)_5]_2$. From EPR spectroscopy and extended Hückel MO calculations the authors were able to show that, in fact, a μ_2-bridging thiyl radical is formed where the unpaired electron resides "to a large extent in a p-type orbital on the trigonal sulfur, which is π-conjugated to d orbitals of the neighboring Cr atoms". Mononuclear $[(CO)_5CrSR]^o$ species have a half-life of ~50 μs and even the above dinuclear complex has only limited thermal stability.

In contrast, the stable paramagnetic $[CpMn(CO)_2(SR)]$ species ($S = {}^1/_2$) described by Huttner et al.[14] are probably best described as low-spin (thiolato)manganese(II) species rather than (thiyl)-manganese(I) since the large ^{55}Mn hyperfine coupling constants of 50−56 G are not compatible with a Mn^I-$\dot{S}R$ formulation; they resemble closely those reported for other low-spin Mn(II) complexes of this type.[15]

To generate, if possible, (thiyl)metal complexes with a biologically more relevant coordination sphere comprising redox-innocent, O,N-spectator ligands, we have synthesized a series of pendent arm macrocycles $[L^1]^{3-}$, $[L^2]^{3-}$, $[L^3]^{3-}$, the structures of which are shown in Scheme 1. These ligands contain a redox-stable 1,4,7-triazacyclononane-1,4-diacetate backbone and a third, potentially redox-active phenolate or thiophenolate pendent arm. As these trianionic ligands are hexadentate, they are expected to form extremely stable mononuclear neutral complexes, $[M^{III}L]$, with trivalent metal ions such as gallium(III), iron(III), and cobalt(III). Electrochemical or chemical one-electron oxidations should yield phenoxyl and thiyl species $[M^{III}L^{\bullet}]^+$ which can be studied in solution by spectroscopy (UV−vis, EPR, Mössbauer).

Scheme 1

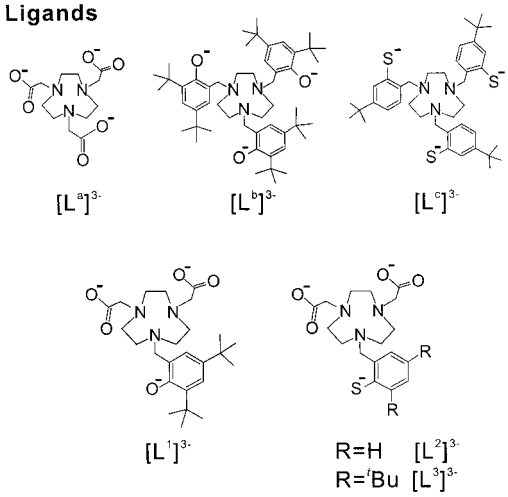

Experimental Section

The solvents diethyl ether, toluene, and *n*-pentane were dried over Na-benzophenone and methanol, ethanol, dichloromethane, chloroform, and tetrachloromethane over CaH_2 and distilled under argon before use. The chemicals α,α′-azoisobutyronitrile (AIBN), bromoacetic acid ethyl ester, 2-*tert*-butoxycarbonyloxyimino-2-phenylacetonitrile (BOC-ON), elemental bromine, 1.6 M *n*-butyllithium in *n*-hexane, trifluoroacetic acid, citric acid, iron powder (ϕ 150 μm), hexamethylenetetramine, mercury diacetate, potassium hydroxide, 1-chloromethyl-4-methoxybenzene, (4-methoxyphenyl)methanethiol, sodium metal, $NaBH_4$, NaOH, *N*-bromosuccinimide (NBS), triethylamine, phosphorustribromide, potassium toluene-4-thiosulfonate, acetone, 1,4-dioxane, *n*-hexane, 2-propanol and dimethylformamide (DMF) were obtained from commercial sources and used without further purification. [1,4,7]Triazonane (1,4,7-triazacyclononane, TACN) and 2-bromomethyl-4,6-di-*tert*-butylphenol were synthesized as described in the literature.[16,17]

[1,4,7]Triazonane-1,4-dicarboxylic acid di-*tert*-butyl Ester (1). To a solution of [1,4,7]triazonane (TACN) (10.0 g, 0.08 mol) in $CHCl_3$ (200 mL) was added triethylamine (32 mL dried over Na_2SO_4) at room temperature. BOC-ON (38.1 g, 0.16 mol) dissolved in $CHCl_3$ (200 mL) was added with stirring within 30 min. The solution was stirred at room temperature for additional 2 h and was then concentrated under reduced pressure. To the obtained residue was added EtOAc (300 mL). The EtOAc solution was successively washed with 4% $NaHCO_3$(aq) (300 mL), NaCl(aq) (300 mL), and 10% citric acid(aq) (3 × 300 mL), whereupon the desired product moved to the aqueous phase. To the aqueous phase was carefully added NaOH under ice-cooling until the pH was adjusted to 10. The turbid solution was extracted with $CHCl_3$ (3 × 200 mL). The organic phase was dried over Na_2SO_4 and concentrated under reduced pressure to give a yellow oil. Upon storage at −30 °C white crystals precipitated. Yield: 18.8 g (74%). ^{1}H NMR (400 MHz, chloroform-d_1): δ 1.42 (s, 18H, CH_3(*t*-Bu)), 2.87 (m, 4H, TACN ring), 3.19 (m, 4H, TACN ring), 3.40 (m, 4H, TACN ring). ^{13}C NMR (100 MHz, chloroform-d_1): δ 28.5 (*t*-Bu), 47.3, 47.7, 48.1, 48.2, 49.5, 49.8, 50.4, 51.6, 52.3, 52.5, 53.0 (TACN ring), 79.6, 79.7 (*t*-Bu), 155.7, 155.9 (C═O). These spectra are very similar to those reported in ref 26b. Especially the ^{13}C NMR spectrum indicates that two conformers of **1** exist in solution. EI mass spectrometry: m/z = 329

(10) Rundel, W. *Chem. Ber.* **1969**, *102*, 359.
(11) (a) Müller, E.; Ley, K. *Chem. Ber.* **1954**, *87*, 922. (b) Cook, C. D.; Woodworth, R. C. *J. Am. Chem. Soc.* **1953**, *75*, 6242. (c) Land, E. J.; Porter, G. *J. Chem. Soc.* **1961**, 3540. (d) Griller, D.; Barclay, L. R. C.; Ingold, K. U. *J. Am. Chem. Soc.* **1975**, *97*, 6151.
(12) (a) Chaudhuri, P.; Wieghardt, K. *Progr. Inorg. Chem.* **2001**. In press. (b) Jazdzewski, B. A.; Tolman, W. B. *Coord. Chem. Rev.* **2000**, *200*−*202*, 633. (c) Goldberg, D. P.; Lippard, S. J. In *Mechanistic Bioinorganic Chemistry;* Thorp, H. H., Pecoraro, V. L., Eds.; Advances in Chemistry Series 246; American Chemical Society: Washington, DC, 1995; p 59. (d) Fontecave, M.; Pierre, J.-L. *Coord. Chem. Rev.* **1998**, *170*, 125.
(13) Springs, J.; Janzen, C. P.; Darensbourg, M. Y.; Calabrese, J. C.; Krusic, P. J.; Verpeaux, J.-N.; Amatore, C. *J. Am. Chem. Soc.* **1990**, *112*, 5789.
(14) Lau, P.; Braunwarth, H.; Huttner, G.; Günauer, D.; Evertz, K.; Imhof, W.; Emmerich, C.; Zsolnai, L. *Organometallics* **1991**, *10*, 3861.
(15) (a) Gross, R.; Kaim, W. *Angew. Chem.* **1985**, *97*, 869; *Angew. Chem., Int. Ed. Engl.* **1985**, *24*, 856. (b) Gross, R.; Kaim, W. *Inorg. Chem.* **1987**, *26*, 3596.
(16) Wieghardt, K.; Schmidt, W.; Nuber, B.; Weiss, J. *Chem. Ber.* **1979**, *112*, 2220.
(17) Sokolowski, A.; Müller, J.; Weyhermüller, T.; Schnepf, R.; Hildebrandt, P.; Hildenbrand, K.; Bothe, E.; Wieghardt, K. *J. Am. Chem. Soc.* **1997**, *119*, 8889.

(M^+). Anal. Calcd for $C_{16}H_{31}N_3O_4$: C, 58.33; H, 9.49; N, 12.76. Found: C, 58.16; H, 9.42; N, 12.75.

7-(3,5-Di-*tert*-butyl-2-hydoxybenzyl)-[1,4,7]triazonane-1,4-dicarboxylic acid di-*tert*-butyl Ester (2). To a solution of **1** (3.8 g, 12 mmol) in toluene (50 mL) was added KOH (1.0 g, 18 mmol) at room temperature. To this mixture was added 2-bromomethyl-4,6-di-*tert*-butylphenol (3.8 g, 13 mmol) in toluene (30 mL) within 10 min. The mixture was stirred at 70 °C for 6 h, filtered and dried over $MgSO_4$, and was concentrated under reduced pressure to give a white powder of **2**. Yield: 6.0 g (95%). ^{1}H NMR (250 MHz, chloroform-d_1): δ 1.25 (9H, CH_3(*t*-Bu)), 1.38 (9H, CH_3(*t*-Bu)), 1.48 (18H, CH_3(*t*-Bu)), 2.76 (br, 4H, TACN ring), 3.33 (br, 4H, TACN ring), 3.45 (br, 4H, TACN ring), 3.84 (2H, NCH_2Ph), 6.83 (1H), 7.18 (1H), 10.2 (br, 1H, OH). ^{13}C NMR (63 MHz, chloroform-d_1): δ 28.5, 28.6, 29.5, 31.6 (CH_3(*t*-Bu)), 34.1, 34.8 (*t*-Bu), 47.6, 48.8, 49.2, 50.4, 52.9 (TACN ring), 61.6 (NCH_2Ph(O)), 79.9, 80.1 (*t*-Bu(BOC)), 121.3, 123.0, 123.7, 135.6, 140.5, 153.9 ($C_{arom.}$), 155.4 (C═O). EI mass spectrometry: m/z = 547 (M^+).

[1-(3,5-Di-*tert*-butyl-2-hydoxybenzyl)-[1,4,7]triazonan-4,7-ium]-bis(trifluoroacetate) (3). To a solution of **2** (6.0 g, 11 mmol) in CH_2Cl_2 (10 mL) was added 50 v/v% CF_3CO_2H/CH_2Cl_2 (60 mL) at 0 °C. This solution was stirred at 0 °C for 30 min and then concentrated under reduced pressure. Et_2O was added to the residue obtained. The solvent was removed by rotary evaporation in order to remove excess CF_3CO_2H. A pale white powder precipitated, which was washed with Et_2O/*n*-pentane (1/1 v/v) and dried under reduced pressure. Yield: 5.6 g (86%). ^{1}H NMR (500 MHz, methanol-d_4): δ 1.28 (s, 9H, CH_3(*t*-Bu)), 1.42 (s, 9H, CH_3(*t*-Bu)), 2.98 (m, 8H, TACN ring), 3.62 (s, 4H, TACN ring), 3.88 (s, 2H, NCH_2Ph), 7.11 (d, 1H, J = 2.4 Hz), 7.32 (d, 1H, J = 2.4 Hz). ^{13}C NMR (126 MHz, methanol-d_4): δ 30.3, 32.0 (CH_3(*t*-Bu)), 35.1, 35.9 (*t*-Bu), 45.0, 46.6, 51.2 (TACN ring), 58.8 (NCH_2Ph(O)), 119.2, 125.1, 127.6, 139.1, 144.2, 152.8 ($C_{arom.}$), 116.9 (CF_3), 163.3 (q, C═O, J = 35 Hz). ESI mass spectrometry indicated CF_3CO_2H free fragment. m/z = 348 ($M' + H)^+$. IR: 1694, 1663 cm^{-1} ν(C═O). Anal. Calcd for $C_{25}H_{41}N_3O_6F_6$: C, 50.58; H, 6.96; N, 7.08. Found: C, 50.72; H, 6.85; N, 7.38.

2,4-Di-*tert*-butyl-6-[1,4,7]triazonan-1-yl-methylphenol (4). To a solution of **3** (5.5 g, 9.3 mmol) in H_2O/CH_3OH (250 mL/50 mL) was slowly added 1 M NaOH(aq) until the pH was adjusted to 9−10. Then the mixture was extracted with $CHCl_3$ (2 × 100 mL). The $CHCl_3$ solution was washed with saturated NaCl(aq) (100 mL), dried over $MgSO_4$, and concentrated under reduced pressure to give a pale yellow-white powder. Yield: 3.0 g (93%). ^{1}H NMR (250 MHz, chloroform-d_1): δ 1.24 (s, 9H, CH_3(*t*-Bu)), 1.37 (s, 9H, CH_3(*t*-Bu)), 2.79 (m, 4H, TACN ring), 2.90 (m, 4H, TACN ring), 2.96 (s, 4H, TACN ring), 3.78 (s, 2H, NCH_2Ph), 6.0 (br), 6.81 (d, 1H, J = 2.4 Hz), 7.19 (d, 1H, J = 2.4 Hz). ^{13}C NMR (63 MHz, chloroform-d_1): δ 29.6, 31.6 (CH_3(*t*-Bu)), 34.1, 34.8 (*t*-Bu), 46.2, 46.7, 52.9 (TACN ring), 61.8 (NCH_2Ph-(O)), 121.8, 123.3, 123.8, 135.9, 141.1, 153.4 ($C_{arom.}$). EI mass spectrometry: m/z = 347 (M^+).

[4-(3,5-Di-*tert*-butyl-2-hydroxybenzyl)-7-ethoxycarbonylmethyl-[1,4,7]triazonan-1-yl]-acetic acid ethyl ester (5). To a solution of **4** (2.9 g, 8.3 mol) in ethanol (30 mL) was added bromoacetic acid ethyl ester (1.9 mL, 17 mmol) at room temperature. Sodium metal (0.4 g, 17 mmol) dissolved in ethanol (40 mL) was added under ice cooling within 10 min. The mixture was stirred at 0 °C for 1 h. A white powder was filtered off, and the filtrate was concentrated under reduced pressure. Toluene was added to the residue, and the mixture was stirred at room temperature for 2 h. A white precipitate was filtered off, and the filtrate was concentrated under reduced pressure. The residue was extracted with *n*-hexane, and the extract was concentrated under reduced pressure to give a yellow oil of **5**. Yield: 2.6 g (60%). ^{1}H NMR (250 MHz, chloroform-d_1): δ 1.21−1.26 (15H, CH_3(*t*-Bu) and Et(CH_3)), 1.39 (s, 9H, CH_3(*t*-Bu)), 2.75 (s, 4H, TACN ring), 2.90 (br, 8H, TACN ring), 3.44 (s, 4H, CH_2CO_2), 3.8 (br, 2H, NCH_2Ph), 4.12 (q, 4H, CH_2-(Et), J = 7 Hz), 6.83 (br, 1H), 7.18 (br, 1H). EI mass spectrometry: m/z = 519 (M^+).

[4-Carboxymethyl-7-(3,5-di-*tert*-butyl-2-hydroxybenzyl)-[1,4,7]-triazonan-1-yl]-acetic acid Li salt ($Li_3[L^1]$). To a solution of **5** (2.6 g, 5.0 mmol) in ethanol (50 mL) was added finely powdered LiOH·H_2O (0.63 g, 15 mmol). The mixture was stirred at 70 °C for 6 h. After which time *n*-hexane/Et_2O (1/1 v/v, 50 mL) was added and stirred at room temperature for 1 h. A white precipitate was collected, washed with Et_2O, and dried. Yield: 2.0 g (83%). ^{1}H NMR (500 MHz, D_2O): δ 1.14 (s, 9H, CH_3(*t*-Bu)), 1.19 (s, 9H, CH_3(*t*-Bu)), 2.13 (br, 4H, TACN ring), 2.36 (br, 8H, TACN ring), 2.95 (br, 4H, NCH_2CO_2), 3.49 (br, 2H, NCH_2Ph), 6.79 (br, 1H), 7.04 (br, 1H). ^{13}C NMR (126 MHz, D_2O): δ 30.0, 31.9 (CH_3(*t*-Bu)), 33.8, 34.4 (*t*-Bu), 52.2, 53.6, 54.0 (TACN ring), 57.4 (**C**H_2CO_2), 60.2 (NCH_2Ph(O)), 122.7, 125.8, 126.5, 137.5, 139.2, 155.2 ($C_{arom.}$), 180.6 (C═O). ESI mass spectrometry in CH_3OH (negative ion mode): m/z = 468 (M − 2Li + H)$^-$, 462 (M − 3Li + 2H)$^-$. Anal. Calcd for $C_{25}H_{38}N_3O_5Li_3$: C, 62.37; H, 7.96; N, 8.73. Found: C, 62.18; H, 8.05; N, 8.55.

2-(4-Methoxybenzylsulfanyl)-benzaldehyde (6). To 120 mL of DMF was added 2-nitrobenzaldehyde (42 g, 0.28 mol) with ice cooling. To the clear solution was added (4-methoxyphenyl)methanethiol (45 g, 0.29 mol) and then K_2CO_3 (50 g, 0.36 mol) at 0 °C. This mixture was stirred at 80 °C for 19 h and then cooled to room temperature. The mixture was added to ice−water (2 L) with stirring. A yellow solid was collected, washed with water, and dried under reduced pressure. This crude solid was recrystallized from $CHCl_3$/petroleum ether. Pale yellow needle-shaped crystals were collected and dried under reduce pressure. Yield: 36 g (50%). ^{1}H NMR (250 MHz, chloroform-d_1): δ 3.74 (s, 3H, OCH_3), 4.06 (s, 2H, CH_2), 6.79 (m, 2H), 7.16 (m, 2H), 7.28 (m, 1H), 7.42−7.46 (m, 2H), 7.78 (m, 1H), 10.2 (s, 1H, CHO). ^{13}C NMR (63 MHz, chloroform-d_1): δ 38.2 (CH_2), 55.2 (OCH_3), 114.0, 125.9, 127.9, 129.8, 130.0, 131.4, 133.8, 134.5, 141.2, 158.9 (C_{arom}), 191.3 (CHO). EI mass spectrometry: m/z = 258 (M^+). Anal. Calcd for $C_{15}H_{14}O_2S$: C, 69.76; H, 5.46; S, 12.39. Found: C, 69.71; H, 5.48; S, 12.40.

[2-(4-Methoxybenzylsulfanyl)-phenyl]-methanol (7). To a solution of **6** (10 g, 39 mmol) in 2-propanol (300 mL) was added $NaBH_4$ (1.2 g, 32 mmol) at room temperature. The mixture was stirred at room temperature for 2 h and concentrated under reduced pressure. To the residue were added 100 mL of Et_2O and 500 mL of saturated NaCl-(aq). The Et_2O solution was collected, and the aqueous phase was extracted with Et_2O (2 × 100 mL). The organic phases were combined and washed with saturated NaCl(aq) (3 × 500 mL). Then the Et_2O phase was dried over $MgSO_4$ and concentrated. A pale yellow-white crystalline solid was collected and dried under reduced pressure. Yield: 10 g (99%). ^{1}H NMR (250 MHz, chloroform-d_1): δ 2.28 (br, 1H, OH), 3.75 (s, 3H, OCH_3), 4.02 (s, 2H, CH_2), 4.63 (s, 2H, C**H**$_2$-OH), 6.79 (m, 2H), 7.17 (m, 2H), 7.21−7.24 (m), 7.34−7.37 (m). ^{13}C NMR (63 MHz, chloroform-d_1): δ 39.1 (CH_2), 55.1 (OCH_3), 63.4 (CH_2-OH), 113.8, 127.1, 128.1, 128.2, 129.2, 129.8, 131.4, 134.2, 141.5, 158.7 (C_{arom}). EI mass spectrometry: m/z = 260 (M^+). Anal. Calcd for $C_{15}H_{16}O_2S$: C, 69.21; H, 6.20; S, 12.29. Found: C, 69.07; H, 6.22; S, 12.31.

1-Bromomethyl-2-(4-methoxybenzylsulfanyl)-benzene (8). To a solution of **7** (8.8 g, 34 mmol) in 100 mL of $CHCl_3$ was added PBr_3 (2.2 mL, 23 mmol) in 50 mL of $CHCl_3$ under ice cooling within 25 min. The solution was stirred at 0 °C for 30 min. Subsequently, the solution was washed with saturated NaCl(aq) (3 × 500 mL). The organic phase was dried over $MgSO_4$ and concentrated under reduced pressure to give a pale yellow crystalline solid. The crystals were collected, washed with *n*-hexane, and dried under reduced pressure. Yield: 4.8 g (44%). ^{1}H NMR (400 MHz, chloroform-d_1): δ 3.77 (s, 3H, OCH_3), 4.08 (s, 2H, CH_2), 4.60 (s, 2H, CH_2Br), 6.80 (d, 2H, J = 8.6 Hz), 7.20 (m, 4H), 7.36 (t, 2H, J = 7.4 Hz). ^{13}C NMR (100 MHz, chloroform-d_1): δ 32.1 (CH_2), 39.0 (CH_2S), 55.2 (OCH_3), 113.9, 127.2, 129.0, 129.1, 130.0, 130.5, 132.0, 136.2, 138.5, 158.8 (C_{arom}). EI mass spectrometry: m/z = 322 (M^+). Anal. Calcd for $C_{15}H_{15}OSBr$: C, 55.74; H, 4.68; S, 9.90; Br, 24.72. Found: C, 55.61; H, 4.77; S, 9.91; Br, 24.69.

7-[2-(4-Methoxybenzylsulfanyl)-benzyl]-[1,4,7]triazonane-1,4-dicarboxylic Acid Di-*tert*-butyl Ester (9). To a solution of **1** (4.3 g, 13 mmol) in toluene (50 mL) was added **8** (4.7 g, 15 mmol) dissolved in toluene (60 mL) under ice cooling. Finely powdered KOH (2.4 g, 43 mmol) was added to the solution. This mixture was stirred at 80 °C for 24 h and then cooled to room temperature and dried over $MgSO_4$ and filtered. The filtrate was concentrated under reduced pressure to give a yellow oil. Yield: 7.0 g (94%). This oil was used for the

following synthesis. ^{1}H NMR (250 MHz, chloroform-d_1): δ 1.39 (s, 9H, CH_3(*t*-Bu)), 1.46 (s, 9H, CH_3(*t*-Bu)), 2.5−3.5 (m, 12H, TACN ring), 3.70 (s, 2H, CH_2N), 3.74 (s, 3H, OCH_3), 3.99 (2H, SCH_2), 6.78 (m), 7.0−7.4 (m). ^{13}C NMR (63 MHz, chloroform-d_1): δ 28.4, 28.5, 38.3, 49.0, 49.1, 49.4, 49.9, 50.1, 50.3, 50.8, 53.4, 53.7, 54.2, 55.2, 58, 79.3, 79.4, 113.8, 126.0, 127.2, 129.2, 129.4, 129.7, 129.9, 136, 139, 155.4, 155.6, 158.7. EI mass spectrometry: m/z = 571 (M^+).

{**4-[2-(4-Methoxybenzylsulfanyl)-benzyl]-[1,4,7]triazonan-1,4,7-ium**} **Trifluoroacetate (10).** To a solution of **9** (6.9 g, 12 mmol) in CH_2Cl_2 (50 mL) was added 50 mL of CF_3CO_2H at 0 °C. The solution was stirred at 0 °C for 30 min and then concentrated under reduced pressure, yielding a red-brown residue from which a pale yellow-white powder precipitated upon addition of Et_2O. This powder was collected, washed with Et_2O, and dried in air. The purity of this powder was confirmed by GC analysis (90% purity). Yield: 5.3 g (62%). ^{1}H NMR (250 MHz, chloroform-d_1): δ 2.90, 3.05, 3.58 (br, 12H, TACN ring), 3.71 (s, 3H, OCH_3), 3.82 (br, 2H, NCH_2Ph), 3.99 (br, 2H, SCH_2), 6.75 (d, 2H, J = 8.6 Hz), 7.07 (d, 2H, J = 8.6 Hz), 7.2−7.4 (m), 8.5 (br). ^{13}C NMR (63 MHz, chloroform-d_1): δ 38.7 (SCH_2), 42.8, 44.5, 49.2 (TACN ring), 55.1 (OCH_3), 56.7 (NCH_2Ph), 113.9, 126.8, 128.7, 128.8, 129.8, 130.7, 130.9, 136.0, 136.3, 158.9 (C_{arom}), 118.8 (CF_3), 162.1 (q, C═O, 35 Hz). FAB mass spectrometry (negative ion mode, matrix: dimethoxybenzyl alcohol): m/z = 712 $(M-H)^-$. IR: 1678 cm^{-1} ν-(C═O).

1-[2-(4-Methoxybenzylsulfanyl)-benzyl]-[1,4,7]triazonane (11). To a solution of **10** (5.0 g, 7.0 mmol) in 100 mL of water was added 1 M NaOH(aq) under ice cooling until a pH value of ca. 10−12 was obtained. To this mixture was added 100 mL of $CHCl_3$, and the $CHCl_3$ layer was collected. The aqueous phase was extracted with $CHCl_3$ (2 × 100 mL). The combined organic phases were washed with saturated NaCl(aq) (3 × 300 mL). The $CHCl_3$ solution was dried over $MgSO_4$, filtered, and concentrated under reduced pressure. The residue was washed with Et_2O and *n*-hexane and dried under reduced pressure to give a pale yellow powder. The purity of this powder was checked by GC analysis (81% purity). Yield: 2.4 g (92%). ^{1}H NMR (250 MHz, chloroform-d_1): δ 2.65 (m, 8H, TACN ring), 2.95 (br, 4H, TACN ring), 3.69 (s, 2H, NCH_2Ph), 3.72 (s, 3H, OCH_3), 4.09 (s, 2H, CH_2S), 4.9 (br), 6.7−7.3 (H_{arom}). ^{13}C NMR (63 MHz, chloroform-d_1): δ 37.6 (SCH_2), 43.4, 44.8, 50.3 (TACN ring), 55.2 (OCH_3), 59.7 (NCH_2), 113.8, 125.7, 128.4, 128.9, 129.2, 129.9, 130.1, 137.0, 137.1, 158.7 ($C_{arom.}$). EI mass spectrometry: m/z = 371 (M^+).

{**4-Ethoxycarbonylmethyl-7-[2-(4-methoxybenzylsulfanyl)-benzyl]-[1,4,7]triazonan-1-yl**}**-acetic acid ethyl ester (12).** To a solution of **11** (2.9 g, 7.8 mmol) in ethanol (30 mL) was added bromoacetic acid ethyl ester (1.8 mL, 16 mmol) at room temperature. The solution was cooled to 0 °C, and sodium metal (0.37 g, 16 mmol) dissolved in ethanol (40 mL) was added and stirred at 0 °C for 30 min. A white precipitate was filtered off, and the filtrate was concentrated under reduced pressure. To this residue was added 50 mL of toluene, and the mixture was stirred for 2 h. Solid NaBr was removed by filtration, and the filtrate was concentrated under reduced pressure to give a yellow oil, which was extracted with Et_2O. The Et_2O solution was concentrated, and the obtained residue was dried under reduced pressure. Yield: 2.6 g (61%). This product was used without further purification. ^{1}H NMR (400 MHz, chloroform-d_1): δ 1.23 (t, 6H, CH_3(Et), J = 7 Hz), 2.74 (br, 4H, TACN ring), 2.80, (br, 4H, TACN ring), 2.88 (br, 4H, TACN ring), 3.35 (s, 4H, NCH_2CO_2), 3.66 (s, 2H, NCH_2Ph), 3.74 (s, 3H, OCH_3), 4.01 (s, 2H, CH_2S), 4.11 (q, 4H, CH_2(Et), J = 7 Hz), 6.77 (m 2H), 7.11−7.17 (m, 4H), 7.29 (m, 1H), 7.39 (br, 1H). ^{13}C NMR (100 MHz, chloroform-d_1): δ 14.3 (CH_3(Et)), 38.3 (SCH_2), 55.2 (OCH_3), 55.0, 55.3, 55.7 (TACN ring), 58.8 (NCH_2CO_2), 60.1 (NCH_2Ph(S) and CH_2(Et)), 113.8, 125.7, 127.1, 129.2, 129.4, 129.7, 129.9, 136.5, 139.9, 158.7 ($C_{arom.}$), 172.1 (C═O). EI mass spectrometry: m/z = 543 (M^+).

{**4-Carboxymethyl-7-[2-(4-methoxybenzylsulfanyl)-benzyl]-[1,4,7]-triazonan-1-yl**}**-acetic Acid Li Salt (13).** To a solution of **12** (2.4 g, 4.4 mmol) in ethanol (30 mL) was added finely powdered $LiOH\cdot H_2O$ (0.37 g, 8.8 mmol). The mixture was stirred at 70 °C for 17 h and filtered. The filtrate was concentrated under reduced pressure to give a pale yellow solid. This solid was washed with Et_2O and dried under reduced pressure. Yield: 2.1 g (95%). ^{1}H NMR (400 MHz, chloroform-d_1): δ 2.32, 2.47, 2.65 (br, 12H, TACN ring), 3.11 (br, 4H, NCH_2-CO_2), 3.42 (s, 2H, NCH_2Ph), 3.72 (s, 3H, OCH_3), 3.95 (s, 2H, SCH_2), 6.74 (d, 2H, J = 8.5 Hz), 7.05−7.24 (m, 5H), 7.47 (br, 1H). ^{13}C NMR (100 MHz, chloroform-d_1): δ 38.5 (SCH_2), 50.4 (NCH_2Ph (S)), 52.4, 52.5, 53.1 (TACN ring), 55.2 (OCH_3), 62.6 (NCH_2CO_2), 113.9, 128.1, 129.0, 129.8, 130.0, 132.2, 132.4, 136.5, 158.8 ($C_{arom.}$), 179.1 (C═O). ESI mass spectrometry in CH_3OH (negative ion mode): m/z = 492 $(M - Li)^-$, 486 $(M - 2Li + H)^-$.

[4-Carboxymethyl-7-(2-mercaptobenzyl)-[1,4,7]triazonan-1-yl]-acetic Acid Li Salt ($Li_2[L^2H]$). To a solution of **13** (0.3 g, 0.6 mmol) in methanol (3 mL) was added $Hg(OAc)_2$ (0.4 g, 1.3 mmol) at room temperature. The mixture was stirred at 60 °C for 6 h and concentrated under reduced pressure. The pale yellow residue was washed with *n*-pentane (2 × 10 mL) to give a white powder. To this white powder was added 10 mL of methanol. H_2S gas was bubbled through the solution for 20 min and then argon gas for 30 min. Black HgS was filtered off, and the filtrate was concentrated under reduced pressure to give a white powder. Yield 0.22 g. This compound was used for synthesis of metal complexes without further purification. ESI mass spectrometry in CH_3OH (negative ion mode): m/z = 388 $(M - 2Li + Na)^-$.

2-Bromo-1,5-di-*tert*-butyl-3-methylbenzene (14). To a mixture of 1,3-di-*tert*-butyl-5-methylbenzene (20 g, 0.10 mol) and Fe powder (1.2 g, 0.021 mol) in 200 mL of CCl_4 was added Br_2 (5.0 mL, 0.10 mol) in 50 mL of CCl_4 under ice cooling over 2 h. The mixture was stirred at 0 °C for 2 h and filtered. The filtrate was washed with 10% $NaHCO_3$-(aq) (3 × 300 mL) and saturated NaCl(aq) (3 × 300 mL). The organic phase was dried over Na_2SO_4 and concentrated under reduced pressure to give a pale yellow oil. The crude oil was distilled under reduced pressure (144.5−145.5 °C/5−6 mmHg). Yield: 18 g (65%). Colorless oil. ^{1}H NMR (250 MHz, chloroform-d_1): δ 1.38 (s, 9H, CH_3(*t*-Bu)), 1.62 (s, 9H, CH_3(*t*-Bu)), 2.52 (s, 3H, CH_3), 7.21 (d, 1H, J = 2.4 Hz), 7.41 (d, 1H, J = 2.4 Hz). ^{13}C NMR (63 MHz, chloroform-d_1): δ 25.7 (CH_3), 30.2 (CH_3(*t*-Bu)), 31.3 (CH_3(*t*-Bu)), 34.6 (*t*-Bu), 37.3 (*t*-Bu), 122.6, 122.9, 125.9, 139.2, 147.4, 149.2 ($C_{arom.}$). EI mass spectrometry: m/z = 282 (M^+). Anal. Calcd for $C_{15}H_{23}Br$: C, 63.61; H, 8.19; Br, 28.21. Found: C, 63.51; H, 8.24; Br, 28.33.

2-Bromo-3,5-di-*tert*-butylbenzaldehyde (15). To a solution of **14** (60 g, 212 mmol) in CCl_4 (500 mL) was added NBS (42 g, 236 mmol) and AIBN (1.4 g, 8.5 mmol). The reaction mixture was gently heated and then refluxed at 100 °C for 1 h and filtered at −10 °C. The filtrate was concentrated under reduced pressure to give 2-bromo-1-bromomethyl-3,5-di-*tert*-butylbenzene. This compound was used without further purification. ^{1}H NMR (250 MHz, chloroform-d_1): δ 1.38 (s, 9H, CH_3-(*t*-Bu)), 1.62 (s, 9H, CH_3(*t*-Bu)), 4.76 (s, 2H, CH_2Br), 7.41 (d, 1H, J = 2.4 Hz), 7.53 (d, 1H, J = 2.5 Hz). ^{13}C NMR (63 MHz, chloroform-d_1): δ 30.1, 31.1 (CH_3(*t*-Bu)), 34.6, 37.4 (*t*-Bu), 36.5 (CH_2Br), 122.1, 125.8, 126.4, 138.1, 148.3, 149.9.

To the solution of the above 2-bromo-1-bromomethyl-3,5-di-*tert*-butylbenzene in 500 mL of $CHCl_3$ was added hexamethylenetetramine (84 g, 599 mmol). The solution was refluxed at 70−80 °C for 24 h and concentrated under reduced pressure. To the pale yellow residue was added hexamethylenetetramine (84 g, 599 mmol) and 500 mL of 50% CH_3CO_2H(aq). The mixture was heated at 100−110 °C for 24 h, after which time 100 mL of concentrated HCl(aq) was added. The mixture was heated at 100−110 °C for 15 min and then cooled to 25 °C and extracted with Et_2O (3 × 200 mL). The Et_2O solution was successively washed with 2 M HCl(aq) (3 × 500 mL) and saturated NaCl(aq) (3 × 500 mL). The organic phase was dried over Na_2SO_4 and concentrated under reduced pressure to give a reddish yellow oil. The crude oil was purified by column chromatography (Silica gel 60, eluent: *n*-hexane/Et_2O 100/1 (v/v)). Yield: 34−42% (pale yellow oil). ^{1}H NMR (400 MHz, chloroform-d_1): δ 1.30 (s, 9H, CH_3(*t*-Bu)), 1.55 (s, 9H, CH_3(*t*-Bu)), 7.73 (quasi-*d*, 2H), 10.5 (s, 1H, CHO). ^{13}C NMR (100 MHz, chloroform-d_1): δ 30.1, 31.0 (CH_3(*t*-Bu)), 34.8, 37.4 (*t*-Bu), 124.5, 124.9, 131.0, 135.3, 148.4, 150.3 ($C_{arom.}$), 193.9 (CHO). EI mass spectrometry: m/z = 296 (M^+). Anal. Calcd for $C_{15}H_{21}OBr$: C, 60.61; H, 7.12; Br, 26.88. Found: C, 60.40; H, 7.26; Br, 26.80.

(2-Bromo-3,5-di-*tert*-butylphenyl)-methanol (16). To a solution of **15** (21 g, 71 mmol) in 2-propanol (400 mL) was added $NaBH_4$ (2.2 g, 58 mmol) at room temperature. The mixture was stirred at room temperature for 2 h and concentrated under reduced pressure. The

residue was extracted with Et_2O (3 × 200 mL). The collected extracts were washed with saturated NaCl(aq) (3 × 500 mL), dried over Na_2SO_4, and concentrated under reduced pressure yielding pure white crystals. Yield: 18.4 g (87%). ^{1}H NMR (250 MHz, chloroform-d_1): δ 1.32 (s, 9H, CH_3(*t*-Bu)), 1.54 (s, 9H, CH_3(*t*-Bu)), 2.37 (s, 1H, OH), 4.76 (br, 2H, CH_2), 7.36 (d, 1H, J = 2.5 Hz), 7.44 (d, 1H, J = 2.5 Hz). ^{13}C NMR (63 MHz, chloroform-d_1): δ 30.1, 31.3 (CH_3(*t*-Bu)), 34.8, 37.3 (*t*-Bu), 66.9 (CH_2), 120.4, 124.3, 124.7, 140.8, 147.5, 149.9 ($C_{arom.}$). EI mass spectrometry: m/z = 298 (M^+). Anal. Calcd for $C_{15}H_{23}OBr$: C, 60.20; H, 7.75; Br, 26.70. Found: C, 60.38; H, 7.82; Br, 26.53.

Alternatively, **16** was prepared as follows. To the described 2-bromo-1-bromomethyl-3,5-di-*tert*-butylbenzene (66.0 g, 0.18 mol) in 1,4-dioxane (530 mL) was added NaOH (13.2 g, 0.33 mol) in water (550 mL). This mixture was refluxed at 115 °C for 9 h, and Et_2O (500 mL) was added. The Et_2O solution was washed with 2 M HCl(aq) (3 × 500 mL) and saturated NaCl(aq) (3 × 500 mL). The Et_2O phase was dried over $MgSO_4$ and concentrated under reduced pressure to give a pale yellow oil. This crude oil was purified by column chromatography (Merck Silica gel 60, eluent: *n*-hexane/Et_2O 10/3 (v/v)). White crystals. Yield: 32.1 g (59%).

Toluene-4-thiosulfonic Acid *S*-(4-Methoxybenzyl) Ester (17). To a solution of 1-chloromethyl-4-methoxybenzene (15.0 g, 0.10 mol) in acetone (75 mL) was added potassium toluene-4-thiosulfonate (22.5 g, 0.10 mol) dissolved in acetone (200 mL). The mixture was refluxed at 70 °C for 8 h, filtered, and concentrated under reduced pressure. The residue obtained was extracted with Et_2O (3 × 100 mL), and a colorless precipitate was filtered off. The Et_2O solution was washed with saturated NaCl(aq) (3 × 300 mL) and dried over Na_2SO_4. Removal of the solvent yielded a crude residue, which was recrystallized from CH_3OH, affording colorless crystals. Yield: 22.8 g (77%). ^{1}H NMR (250 MHz, chloroform-d_1): δ 2.41 (s, 3H, CH_3Ph), 3.73 (s, 3H, OCH_3), 4.18 (s, 2H, CH_2), 6.73 (m, 2H), 7.07 (m, 2H), 7.25 (m, 2H), 7.71 (m, 2H). ^{13}C NMR (63 MHz, chloroform-d_1): δ 21.5 (CH_3), 39.8 (CH_2), 55.2 (OCH_3), 114.1, 125.2, 126.9, 129.7, 130.3, 142.0, 144.5, 159.3 ($C_{arom.}$). EI mass spectrometry: m/z = 308 (M^+). Anal. Calcd for $C_{15}H_{16}O_3S_2$: C, 58.44; H, 5.23; S, 20.76. Found: C, 58.56; H, 5.28; S, 20.72.

[3,5-Di-*tert*-butyl-2-(4-methoxybenzylsulfanyl)-phenyl]-methanol (18). To a solution of **16** (17.6 g, 59 mmol) in 100 mL of Et_2O was added 1.6 M *n*-BuLi in *n*-hexane (79.2 mL, 127 mmol) under an argon atmosphere with ice cooling. The solution was stirred at 0 °C for 10 min and then at room temperature for 3 h. To the pale yellow solution was added **17** (18.5 g, 60 mmol) in 200 mL of Et_2O at −70 °C and 30 mL of Et_2O was added. The solution was stirred at −70 °C for 1 h and then at ca. −30 °C for 4 h. To the mixture was added 2 M HCl(aq) (500 mL), and the Et_2O layer was collected. The aqueous phase was extracted with Et_2O (2 × 200 mL). The organic phases were combined and washed with 2 M HCl(aq) (2 × 500 mL) and saturated NaCl(aq) (3 × 500 mL). The solution was dried over Na_2SO_4 and concentrated under reduced pressure to give a crude oil. This oil was purified by column chromatography (Merck Silica gel 60, eluent: *n*-hexane/Et_2O 10/5 (v/v) or toluene/Et_2O 10/1 (v/v)). Yield: 8.6 g (39%). ^{1}H NMR (250 MHz, chloroform-d_1): δ 1.32 (s, 9H, CH_3(*t*-Bu)), 1.58 (s, 9H, CH_3(*t*-Bu)), 2.68 (t, 1H, OH, J = 6.5 Hz), 3.79 (s, 3H, OCH_3), 3.86 (s, 2H, CH_2), 4.97 (d, 2H, C**H**$_2$OH, J = 6.4 Hz), 6.84 (m, 2H), 7.21 (m, 2H), 7.37 (d, 1H, J = 2.2 Hz), 7.46 (d, 1H, J = 2.3 Hz). ^{13}C NMR (63 MHz, chloroform-d_1): δ 31.2, 31.6 (CH_3(*t*-Bu)), 34.9, 37.7 (*t*-Bu), 42.8 (SCH_2), 55.3 (OCH_3), 65.5 (CH_2OH), 114.1, 123.9, 124.5, 129.0, 129.2, 130.1, 146.8, 151.7, 153.8, 158.9 ($C_{arom.}$). EI mass spectrometry: m/z = 372 (M^+). Anal. Calcd for $C_{23}H_{32}O_2S$: C, 74.16; H, 8.66; S, 8.59. Found: C, 73.99; H, 8.68; S, 8.75.

1-Bromomethyl-3,5-di-*tert*-butyl-2-(4-methoxybenzylsulfanyl)-benzene (19). To a solution of **18** (2.5 g, 6.7 mmol) in $CHCl_3$ (30 mL) was added PBr_3 (0.83 mL, 8.7 mmol) in $CHCl_3$ (10 mL) over 15 min, and 10 mL of $CHCl_3$ was added. The clear pale yellow solution was stirred at 0 °C for 90 min and washed with NaBr(aq) (4 × 300 mL). The organic phase was dried over Na_2SO_4 and concentrated under reduced pressure to give a pale yellow oil. Yield: 3.1 g. The compound was used without further purification. For analytical measurements the crude product was purified by column chromatography (Merck Silica gel 60, eluent: *n*-hexane/Et_2O 100/2(v/v)). ^{1}H NMR (250 MHz, chloroform-d_1): δ 1.33 (s, 9H, CH_3(*t*-Bu)), 1.59 (s, 9H, CH_3(*t*-Bu)), 3.80 (s, 3H, OCH_3), 3.98 (s, 2H, SCH_2), 5.03 (s, 2H, CH_2Br), 6.85 (m, 2H), 7.24 (m, 2H), 7.47 (m, 2H). ^{13}C NMR (63 MHz, chloroform-d_1): δ 31.2, 31.6 (CH_3(*t*-Bu)), 34.6 (CH_2Br), 34.9, 37.9 (*t*-Bu), 42.5 (SCH_2), 55.3 (OCH_3), 114.0, 124.8, 126.9, 129.1, 130.2, 130.8, 143.9, 151.7, 153.9, 158.9 ($C_{arom.}$). EI mass spectrometry: m/z = 434 (M^+). Anal. Calcd for $C_{23}H_{31}OBrS$: C, 63.45; H, 7.18; Br, 18.35; S, 7.35. Found: C, 64.44; H, 7.31; Br, 18.03; S, 7.05.

7-[3,5-Di-*tert*-butyl-2-(4-methoxybenzylsulfanyl)-benzyl]-[1,4,7]-triazonane-1,4-dicarboxylic Acid Di-*tert*-butyl Ester (20). To a solution of **1** (2.5 g, 7.6 mmol) in toluene (30 mL) was added **19** (3.7 g, 8.5 mmol) in toluene (35 mL) under ice cooling over 10 min. Finely powdered KOH (1.4 g, 25 mmol) was added to the solution. The mixture was stirred at 80 °C for 24 h and cooled to 25 °C, dried over $MgSO_4$, and filtered. The filtrate was concentrated under reduced pressure to give a yellow solid. Yield: 5.2 g (100%). This solid was used without further purification. EI mass spectrometry: m/z = 683 (M^+). Anal. Calcd for $C_{39}H_{61}N_3O_5S$: C, 68.49; H, 8.99; N, 6.14; S, 4.68. Found: C, 68.52; H, 8.93; N, 6.03; S, 4.79.

{**4-[3,5-Di-*tert*-butyl-2-(4-methoxybenzylsulfanyl)-benzyl]-[1,4,7]-triazonan-1,4,7-ium**} **Trifluoroacetate (21).** To a CF_3CO_2H/CH_2Cl_2 (50 v/v%) solution (60 mL) was added **20** (4.5 g, 6.6 mmol) at 0 °C. The solution was stirred at 0 °C for 30 min and concentrated under reduced pressure. To the red-brown residue was added an *n*-hexane/Et_2O mixture and the solvent was evaporated under reduced pressure. This procedure was repeated to remove excess CF_3CO_2H. To the residue was added an *n*-hexane/Et_2O mixture. After stirring at room temperature a yellow-white powder was obtained. Yield: 3.8 g (70%). ^{1}H NMR (250 MHz, chloroform-d_1): δ 1.28 (s, 9H, CH_3(*t*-Bu)), 1.52 (s, 9H, CH_3(*t*-Bu)), 2.93 (br, 4H, TACN ring), 3.10 (br, 4H, TACN ring), 3.58 (br, 4H, TACN ring), 3.66 (s, 2H, NCH_2Ph), 3.73 (s, 3H, OCH_3), 4.15 (s, 2H, SCH_2), 6.76 (d, 2H, J = 8.5 Hz), 7.02 (d, 2H, J = 8.5 Hz), 7.21 (br, 1H), 7.47 (br, 1H), 8.6 (br). ^{13}C NMR (63 MHz, chloroform-d_1): δ 31.1, 31.5 (CH_3(*t*-Bu)), 34.7, 37.7 (*t*-Bu), 42.6 (SCH_2), 43.9, 44.2, 48.3 (TACN ring), 55.2 (OCH_3), 56.7 (NCH_2), 114.0, 124.4, 126.3, 128.6, 130.0, 131.2, 140.5, 151.8, 154.3, 159.0 ($C_{arom.}$), 118.4 (CF_3), 161.7 (q, C═O, J = 37 Hz). ESI mass spectrometry (acetone): m/z = 484 ($M' + H$)$^+$. IR: 1679 cm^{-1} ν(C═O). Anal. Calcd for $C_{35}H_{48}N_3O_7F_9S$: C, 50.91; H, 5.86; N, 5.09; F, 20.71; S, 3.88. Found: C, 51.12; H, 5.95; N, 5.10; F, 20.92; S, 3.78.

1-[3,5-Di-*tert*-butyl-2-(4-methoxybenzylsulfanyl)-benzyl]-[1,4,7]-triazonane (22). To a solution of **21** (3.6 g, 4.4 mmol) in $CHCl_3$ (100 mL) were added 3.0 mL of NEt_3 with ice cooling. After stirring at 0 °C for 30 min, the organic phase was washed with NaCl(aq) (3 × 300 mL), dried over $MgSO_4$ and concentrated under reduced pressure to give a pale yellow-white powder. The purity of this powder was checked by GC analysis (83% purity). Yield: 1.9 g (90%). ^{1}H NMR (250 MHz, chloroform-d_1): δ 1.29 (s, 9H, CH_3(*t*-Bu)), 1.53 (s, 9H, CH_3(*t*-Bu)), 2.65 (br, 8H, TACN ring), 2.84 (br, 4H, TACN ring), 3.68 (s, 2H, NCH_2Ph), 3.76 (s, 3H, OCH_3), 4.03 (s, 2H, SCH_2), 6.79 (m, 2H), 7.11 (m, 2H,), 7.37 (quasi-*d*, 1H), 7.42 (quasi-*d*, 1H). ^{13}C NMR (63 MHz, chloroform-d_1): δ 31.3, 31.6 (CH_3(*t*-Bu)), 34.8, 37.6 (*t*-Bu), 42.9 (SCH_2), 45.5, 45.8, 52.0 (TACN ring), 55.2 (OCH_3), 59.4 (NCH_2), 113.9, 123.1, 125.4, 129.4, 130.0, 130.7, 144.6, 150.9, 153.4, 158.8 ($C_{arom.}$). EI mass spectrometry: 483 (M^+).

{**4-Carboxymethyl-7-[3,5-di-*tert*-butyl-2-(4-methoxybenzylsulfanyl)-benzyl]-[1,4,7]triazonan-1-yl**}**-acetic Acid Li Salt (23).** To a solution of **22** (1.9 g, 3.9 mmol) in ethanol (30 mL) was added bromoacetatic acid ethyl ester (0.9 mL, 8.1 mmol) at room temperature. The solution was cooled at 0 °C. Sodium metal (0.19 g, 8.3 mmol) dissolved in ethanol (20 mL) was added at 0 °C over 5 min. After stirring at 0 °C for 30 min, the solution was concentrated under reduced pressure to give a pale yellow-white residue. To this residue was added toluene (50 mL), and the mixture was stirred for 90 min and filtered. The filtrate was concentrated under reduced pressure to give a yellow oil to which was added *n*-hexane, and a white powder was removed by filtration. The filtrate was concentrated under reduced pressure to give a crude compound. From NMR and mass spectrometry, it was established that the crude oil contained ca. 65 wt % of product and ca. 35 wt % di-substituted compound. The crude oil reacted with bromoacetatic acid ethyl ester (0.15 mL) and sodium metal (30 mg).

After the reaction was completed, a pale yellow oil (1.2 g) was obtained and used for the next reaction without further purification. To the oil (1.2 g) in ethanol (30 mL) was added finely powdered $LiOH \cdot H_2O$ (0.16 g, 3.8 mmol) at room temperature. The mixture was stirred at 70 °C for 6 h and filtered. The filtrate was concentrated under reduced pressure to give a yellow oil. To this oil was added an *n*-hexane/Et_2O solution, and the solvent was evaporated to remove ethanol. During this procedure a white powder precipitated. The powder was washed with *n*-pentane, collected, and dried under reduced pressure. Yield: 0.92 g (38%). ESI mass spectrometry in methanol (negative ion mode): m/z = 604 $(M - Li)^-$, 598 $(M - 2Li + H)^-$. IR: 1609, 1594 cm^{-1} ν(C=O).

[4-Carboxymethyl-7-(3,5-di-*tert*-butyl-2-mercaptobenzyl)-[1,4,7]-triazonan-1-yl]-acetic Acid Li Salt (HLi_2L^3). The synthesis of this compound was performed under an atmosphere of argon. To **23** (0.20 g, 0.33 mmol) and $Hg(CH_3CO_2)_2$ (0.22 g, 0.69 mmol) was added methanol (10 mL). The solution was stirred at 60 °C for 6 h and then concentrated under reduced pressure. The residue was washed with *n*-pentane (2 × 10 mL) and dried under reduced pressure to give a white powder. To the powder was added methanol (10 mL). Through this suspension was bubbled H_2S gas for 20 min and then argon for 30 min. Black HgS was filtered off, and the colorless filtrate was concentrated under reduced pressure to give a white powder. Yield: 0.20 g. This powder was used for synthesis of metal complexes without further purification. ESI mass spectrometry in methanol (negative ion mode): m/z = 478 $(M - 2Li + H)^-$.

Preparation of Complexes. [GaL^1]. To a solution of the ligand Li_3L^1 (118 mg, 0.25 mmol) in CH_3CN (2 mL) was added $GaCl_3$ (41 mg, 0.23 mmol) in CH_3CN (4 mL). The mixture was refluxed at 90 °C for 4 h and concentrated under reduced pressure to give a colorless crude polycrystalline precipitate. The crude crystals were recrystallized from CH_3OH/CH_3CN. Colorless crystals were collected, washed with cold CH_3CN, and dried under reduced pressure. Yield: 88 mg (71%). ^{1}H NMR (500 MHz, methanol-d_4): δ 1.26 (s, 9H, CH_3(*t*-Bu)), 1.35 (s, 9H, CH_3(*t*-Bu)), 2.29 (m, 1H), 2.96 (m, 4H), 3.12 (m, 4H), 3.24 (m, 1H), 3.42 (m, 2H), 3.53 (s, 2H), 3.62 (s, 2H), 3.83 (d, 1H, J = 12 Hz), 4.29 (d, 1H, J = 12 Hz), 6.93 (d, 1H, J = 2.5 Hz), 7.27 (d, 1H, J = 2.6 Hz). ESI mass spectrometry in CH_3OH (positive ion mode): m/z = 552 $(M^0 + Na)^+$ 1083 $(2M^0 + Na)^+$. Anal. Calcd for $C_{25}H_{38}N_3O_5Ga$: C, 56.62; H, 7.22; N, 7.92. Found: C, 56.70; H, 7.29; N, 7.76.

[CoL^1]. A solution of Li_3L^1 (51 mg, 0.11 mmol) and $CoCl_2 \cdot 6H_2O$ (25 mg, 0.11 mmol) in CH_3OH (6 mL) was refluxed at 90 °C under an argon atmosphere for 2 h. Then the solution was refluxed at 90 °C in the presence of air for 2 h. The red-wine colored solution was filtered, and the filtrate was concentrated under reduced pressure. The residue was recrystallized from CH_3OH/acetone. Brown crystals were collected, washed with cold CH_3CN, water, and acetone, and dried under reduced pressure. Yield: 33 mg (60%). Crystals of $[CoL^1] \cdot CH_3OH \cdot 1.5H_2O$ suitable for X-ray crystallography were grown from CH_3OH/CH_3CN by slow evaporation of the solvent. ^{1}H NMR (400 MHz, methanol-d_4): δ 1.25 (s, 9H, CH_3(*t*-Bu)), 1.40 (s, 9H, CH_3(*t*-Bu)), 2.48 (m, 1H), 2.66 (m, 1H), 2.96 (m, 3H), 3.2∼3.4 (m), 3.4∼3.8 (m, 4H), 3.9∼4.1 (m, 3H), 6.90 (d, 1H, J = 2.5 Hz), 7.18 (d, 1H, J = 2.6 Hz). ESI mass spectrometry in CH_3OH (positive ion mode): m/z = 542 $(M^0 + Na)^+$, 1061 $(2M^0 + Na)^+$. Anal. Calcd for $C_{26}H_{45}N_3O_{7.5}Co$: C, 53.97; H, 7.84; N, 7.26. Found: C, 54.49; H, 7.73; N, 7.61.

[FeL^1]. To a solution of Li_3L^1 (53 mg, 0.11 mmol) in CH_3CN (2 mL) was added $FeCl_3$ (21 mg, 0.13 mmol) in CH_3CN (4 mL). The reaction mixture was refluxed at 90 °C for 4 h and concentrated under reduced pressure to give a purple crude solid, which was recrystallized from hot CH_3OH. Purple crystals were collected, washed with cold CH_3OH, and dried under reduced pressure. Yield: 28 mg (49%). Crystals of $[FeL^1] \cdot H_2O$ suitable for X-ray crystallography were obtained from CH_3OH/CH_3CN by slow evaporation of the solvent. ESI mass spectrometry in CH_3OH (positive ion mode): m/z = 539 $(M^0 + Na)^+$, 1055 $(2M^0 + Na)^+$. Anal. Calcd for $C_{25}H_{38}N_3O_5Fe$: C, 58.14; H, 7.42; N, 8.14. Found: C, 58.21; H, 7.49; N, 8.05.

[^{57}FeL^1]. To ^{57}Fe (7.20 mg, 0.13 mmol) was added 30 mL of concentrated HCl(aq), and the mixture was refluxed at 120 °C for 24 h. Then the yellow solution was concentrated under reduced pressure to give yellow $^{57}FeCl_3$. Preparation of the iron complex was performed as described above. Yield 34 mg (52%). ESI mass spectrometry in CH_3OH (positive ion mode): m/z = 540 $(M^0 + Na)^+$, 1057 $(2M^0 + Na)^+$.

[GaL^2]. To HLi_2L^2 (46 mg, 0.13 mmol) in CH_3CN (2 mL) was added a solution of $GaCl_3$ (23 mg, 0.13 mmol) in CH_3CN (4 mL). The mixture was refluxed at 90 °C for 1 h. After addition of 50 μL of NEt_3 the mixture was refluxed at 90 °C for additional 3 h and concentrated under reduced pressure to give a white powder. The crude powder was recrystallized from hot CH_3OH. A white precipitate was collected, washed with cold CH_3CN and Et_2O, and dried under reduced pressure. Yield: 11 mg (20%). ESI mass spectrometry in CH_3OH (positive ion mode): m/z = 456 $(M^0 + Na)^+$, 891 $(2M^0 + Na)^+$. Anal. Calcd for $C_{17}H_{22}N_3O_4SGa$: C, 47.03; H, 5.11; N, 9.68. Found: C, 46.85; H, 5.02; N, 9.73.

[CoL^2]. A solution of HLi_2L^2 (48 mg, 0.13 mmol) and $CoCl_2 \cdot 6H_2O$ (31 mg, 0.13 mmol) in CH_3CN (6 mL) was refluxed at 90 °C for 1 h. 50 μL of NEt_3 were added, and the solution was refluxed at 90 °C under an atmosphere of argon for 1 h and then in the presence of air for 2 h. The solution was concentrated under reduced pressure to give a green solid, which was recrystallized from hot CH_3OH. Red crystals were collected, washed with cold CH_3OH and Et_2O, and dried under reduced pressure. Yield: 15 mg (27%). ESI mass spectrometry in CH_3OH (positive ion mode): m/z = 446 $(M^0 + Na)^+$, 869 $(2M^0 + Na)^+$. Anal. Calcd for $C_{17}H_{22}N_3O_4SCo$: C, 48.23; H, 5.24; N, 9.93. Found: C, 48.16; H, 5.28; N, 10.03.

[FeL^2]. To HLi_2L^2 (45 mg, 0.12 mmol) in CH_3CN (2 mL) was added $FeCl_3$ (20 mg, 0.12 mmol) in CH_3CN (4 mL). The solution was refluxed at 90 °C for 2 h. To this solution was added 50 μL of NEt_3, and the solution was refluxed at 90 °C for additional 2 h and concentrated under reduced pressure to give a greenish blue solid. The crude solid was recrystallized from hot CH_3CN. Black crystals were collected, washed with cold CH_3CN, and dried under reduced pressure. Yield: 8.3 mg (16%). Crystals suitable for X-ray crystallography were grown from methanol. ESI mass spectrometry in CH_3CN (positive ion mode): m/z = 443 $(M^0 + Na)^+$, 863 $(2M^0 + Na)^+$. Anal. Calcd for $C_{17}H_{22}N_3O_4SFe$: C, 48.59; H, 5.28; N, 10.00. Found: C, 48.46; H, 5.22; N, 9.88.

[GaL^3]. To HLi_2L^3 (59 mg, 0.12 mmol) in CH_3OH (6 mL) was added $GaCl_3$ (21 mg, 0.12 mmol) in CH_3OH (4 mL). The mixture was refluxed at 90 °C for 1 h followed by the addition of 50 μL of NEt_3, and the mixture was refluxed at 90 °C for additional 3 h. Subsequently the mixture was filtered under argon, and the filtrate was concentrated to about half the volume, and the solution was stored at −20 °C. A white precipitate was collected, washed with cold CH_3CN, and dried under reduced pressure. Yield: 6 mg (9%). ESI mass spectrometry in CH_3OH (positive ion mode): m/z = 568 $(M^0 + Na)^+$, 584 $(M^0 + K)^+$, 619 $(M^0 + K + 2H_2O)^+$, 647 $(M^0 + K + 2CH_3OH)^+$, 1115 $(2M^0 + Na)^+$. Anal. Calcd for $C_{25}H_{38}N_3O_4SGa \cdot 1\ 1/6H_2O$: C, 52.92; H, 7.17; N, 7.41. Found: C, 52.86; H, 7.30; N, 7.29.

[CoL^3]. A solution of HLi_2L^3 (50 mg, 0.1 mmol) and $CoCl_2 \cdot 6H_2O$ (25 mg, 0.1 mmol) in CH_3CN (4 mL) was refluxed at 90 °C for 1 h. NEt_3 (50 μL) was added, and the mixture was stirred at 90 °C for an additional hour and then at 90 °C in the presence of air for 2 h. The mixture was concentrated under reduced pressure to give a dark green solid. To the solid was added 5.5 mL of CH_3OH, and the color of the solution turned brown. After 2 days at 25 °C, brown, needle-shaped crystals precipitated which were collected, washed with cold CH_3CN, and dried under reduced pressure. Yield: 9 mg (17%). Crystals of $[CoL^3] \cdot 1\ 1/6H_2O$ were suitable for X-ray crystallography. ESI mass spectrometry in CH_3OH (positive ion mode): m/z = 558 $(M^0 + Na)^+$, 1093 $(2M^0 + Na)^+$. Anal. Calcd for $C_{25}H_{38}N_3O_4SCo$: C, 56.07; H, 7.15; N, 7.85. Found: C, 55.94; H, 7.25; N, 7.76.

Physical Measurements. EI, ESI, or FAB mass spectra were recorded on a Finnigan MAT 8200, a Finnigan MAT 95 or a HP 5989 mass spectrometer. ^{1}H and ^{13}C NMR spectra were measured on Bruker ARX 250, DRX 400, or DRX 500 spectrometers using the solvent as internal standard. Electronic absorption spectra were measured in the range 200−1000 nm on a Perkin-Elmer Lambda 19 spectrophotometer. Cyclic voltammograms were measured by use of an EG&G potentiostat/galvanostat 273A on solutions containing 0.1 M $TBA(PF_6)$ as supporting electrolyte in a conventional electrochemical cell. Glassy carbon and Pt wire were used as working and counter electrode, respectively. Potentials were referenced to the Ag/0.01 M $AgNO_3$ CH_3CN or

Table 1. Crystallographic Data for $[FeL^1]\cdot H_2O$, $[CoL^1]\cdot CH_3OH\cdot 1.5\ H_2O$, $[FeL^2]$, $[CoL^3]\cdot 1.17\ H_2O$

	$[FeL^1]\cdot H_2O$	$[CoL^1]\cdot CH_3OH\cdot 1.5\ H_2O$	$[FeL^2]$	$[CoL^3]\cdot 1.17\ H_2O$
chem formula	$C_{25}H_{40}FeN_3O_6$	$C_{26}H_{45}CoN_3O_{7.5}$	$C_{17}H_{22}FeN_3O_4S$	$C_{25}H_{40.33}CoN_3O_{5.17}S$
fw	534.45	578.58	420.29	556.59
space group	$P\bar{1}$, No. 2	$C2/c$, No. 15	$P2_1/n$, No. 14	$P\bar{3}c1$, No. 165
a, Å	12.468(2)	49.743(7)	7.3937(6)	27.694(5)
b, Å	17.667(3)	8.8465(12)	13.8182(12)	27.694(5)
c, Å	25.111(4)	13.293(2)	17.329(2)	13.188(3)
α, deg	79.81(2)	90	90	90
β, deg	79.28(2)	98.90(2)	91.293(12)	90
γ, deg	89.99(2)	90	90	120
V, Å	5346(2)	5779.2(14)	1770.0(3)	8760(3)
Z	8	8	4	12
T, K	100(2)	100(2)	100(2)	100(2)
ρ calcd, g cm^{-3}	1.328	1.330	1.577	1.266
refl. collected/$2\theta_{max}$	27104/45.0	16812/55.0	30347/60.0	13187/35
unique refl/$I > 2\sigma(I)$	13738/8280	6556/4237	5161/4600	1850/924
no. of params/restr	1285/15	356/3	235/0	187/0
μ(Mo Kα), cm^{-1}	6.07	6.42	9.99	6.96
R1[a]	0.0646	0.0544	0.0250	0.0726
wR2[b]($I > 2^{\sigma}(I)$)	0.1576	0.1292	0.0671	0.1652

[a] Observation criterion: $I > 2\sigma(I)$. $R1 = \Sigma||F_o| - |F_c||/\Sigma|F_o|$. [b] $wR2 = [\Sigma[w(F_o^2 - F_c^2)^2]/\Sigma[w(F_o^2)^2]]^{1/2}$ where $w = 1/\sigma^2(F_o^2) + (aP)^2 + bP$, $P = (F_o^2 + 2F_c^2)/3$.

propionitrile solution. Ferrocene was used as internal standard, and potentials were referenced versus the Fc^+/Fc couple. Spectroelectrochemical measurements were performed by using an optically transparent thin-layer electrochemical cell (OTTLE cell). During oxidation/reductions in the OTTLE cell spectral changes were recorded on a Hewlett-Packard HP 8453 diode array spectrophotometer in the range 190−1100 nm. X-band EPR spectra were measured on a Bruker ESP 300 Spectrometer equipped with an Oxford Instruments ESR 910 helium-flow cryostat with an ITC 503 temperature controller. One-electron oxidations of $[^{57}FeL^1]$, $[CoL^1]$, and $[GaL^1]$ were achieved electrochemically in a conventional electrochemical cell by using the following conditions: [complex] = 0.5 mM, $T = -20$ °C. For the electrochemical oxidation of $[CoL^3]$ at −60 °C under an argon atmosphere, a 0.2 mM solution (25 mL) was employed. All samples were immediately frozen in liquid N_2 after the one-electron oxidation and transferred to the respective spectrometer. ^{57}Fe Mössbauer spectra were measured on an Oxford Instruments Mössbauer spectrometer. ^{57}Co/Rh was used as the radiation source. The minimum experimental line widths were 0.24 mms^{-1}. The temperature of the samples was controlled by an Oxford Instruments Variox Cryostat. Isomer shifts were determined relative to α-iron at 300 K.

X-ray Crystallographic Data Collection and Refinement of the Structures. A violet single crystal of $[FeL^1]\cdot H_2O$, and dark brown crystals of $[CoL^1]\cdot CH_3OH\cdot 1.5\ H_2O$ and $[FeL^2]$, and an orange red specimen of $[CoL^3]\cdot 1.17\ H_2O$ were fixed with perfluoropolyether on glass fibers and mounted on a Nonius Kappa-CCD diffractometer equipped with a cryogenic nitrogen cold stream. Graphite monochromated Mo Kα radiation ($\lambda = 0.71073$ Å) was used throughout. Crystallographic data of the compounds are listed in Table 1. Cell constants were obtained from a least-squares fit of the setting angles of several thousand strong reflections. Intensity data were corrected for Lorentz and polarization effects. Intensity data collected from a thin plate-shaped crystal of $[FeL^1]\cdot H_2O$ were corrected for absorption using the program MulScanAbs embedded in the PLATON99 program suite[18] yielding max and min transmission coefficient of 0.92 and 0.77, respectively. The Siemens ShelXTL[19] software package was used for solution, refinement, and artwork of the structures, and neutral atom scattering factors of the program were used. All structures were solved and refined by direct methods and difference Fourier techniques. Non-hydrogen atoms were refined anisotropically except carbon atoms and solvate in compound $[CoL^3]\cdot 1.17\ H_2O$ since the number of observed reflections in the data set was not sufficient to refine all atoms anisotropically. Hydrogen atoms were placed at calculated positions and refined as riding atoms with isotropic displacement parameters. Hydrogen atoms of solvate water molecules in $[FeL^1]\cdot H_2O$ and $[CoL^1]\cdot CH_3OH\cdot 1.5\ H_2O$ were located from the difference map, and O−H distances were restrained to be equal within errors using the SADI instruction in ShelXTL.

(18) Spek, A. L. University of Utrecht, The Netherlands, 1999.
(19) *(19)ShelXTL*, V.5; Siemens Industrial Automation Inc.; 1994.

Results

Preparation of Ligands and Complexes. The hexadentate macrocycles containing a 1,4,7-triazacyclononane backbone and three identical, *N*-bound pendent arms such as acetates, $[L^a]^{3-}$,[20] phenolates, $[L^b]^{3-}$,[21] or thiophenolates, $[L^c]^{3-}$,[22] and their extremely stable,[23] neutral complexes of Ga^{III}, Fe^{III}, and Co^{III} have been thoroughly studied. They serve as benchmarks for the present study where we have synthesized the corresponding *mixed* pendent arm macrocycles $[L^1]^{3-}$, $[L^2]^{3-}$, and $[L^3]^{3-}$ and their octahedral complexes of Ga^{III}, Fe^{III}, and Co^{III}. The structures of the ligands are depicted in Scheme 1.

These mixed pendent arm macrocycles were designed to contain a redox-inert 1,4,7-triazacyclononane-1,4-diacetate[24] unit in addition to one potentially redox-active phenolate or thiophe-

(20) (a) Wieghardt, K.; Bossek, U.; Chaudhuri, P.; Herrmann, W.; Menke, B. C.; Weiss, J. *Inorg. Chem.* **1982**, *21*, 4308. (b) Takahashi, M.; Takamoto, S. *Bull. Chem. Soc. Jpn.* **1977**, *50*, 3413. (c) Arishima, T.; Hamada, K.; Takamoto, S. *Nippon Kagaku Kaishi* **1973**, 1119. (d) Bossek, U.; Hanke, D.; Wieghardt, K.; Nuber, B. *Polyhedron* **1993**, *12*, 1. (e) Craig, A. S.; Parker, D.; Adams, H.; Bailey, N. A. *J. Chem. Soc., Chem. Commun.* **1989**, 1793. (f) Moore, D. A.; Fanwick, P. E.; Welch, M. J. *Inorg. Chem.* **1990**, *29*, 672. (g) Matthews, R. C.; Parker, D.; Ferguson, G.; Kaitner, B.; Harrison, A.; Royle, L. *Polyhedron* **1991**, *10*, 1951. (h) Craig, A. S.; Helps, I. M.; Parker, D.; Adams, H.; Bailey, N. A.; Williams, M. G.; Smith, J. M. A.; Ferguson, G. *Polyhedron* **1989**, *8*, 2481.

(21) (a) Moore, D. A.; Fanwick, P. E.; Welch, M. J. *Inorg. Chem.* **1989**, *28*, 1504. (b) Auerbach, U.; Eckert, U.; Wieghardt, K.; Nuber, B.; Weiss, J. *Inorg. Chem.* **1990**, *29*, 938. (c) Martell, A. E.; Motekaitis, R. J.; Welch, M. J. *J. Chem. Soc., Chem. Commun.* **1990**, 1748. (d) Auerbach, U.; Della Vedova, B. S. P. C.; Wieghardt, K.; Nuber, B.; Weiss, J. *J. Chem. Soc., Chem. Commun.* **1990**, 1004. (e) Auerbach, U.; Stockheim, C.; Weyhermüller, T.; Wieghardt, K.; Nuber, B. *Angew. Chem.* **1993**, *105*, 735; *Angew. Chem., Int. Ed. Engl.* **1993**, *32*, 714. (f) Auerbach, U.; Weyhermüller, T.; Wieghardt, K.; Nuber, B.; Bill, E.; Butzlaff, C.; Trautwein, A. X. *Inorg. Chem.* **1993**, *32*, 508. (g) Clarke, E. T.; Martell, A. E. *Inorg. Chim. Acta* **1991**, *186*, 103.

(22) (a) Beissel, T.; Bürger, K. S.; Voigt, G.; Wieghardt, K.; Butzlaff, C.; Trautwein, A. X. *Inorg. Chem.* **1993**, *32*, 124. (b) Beissel, T.; Glaser, T.; Kesting, F.; Wieghardt, K.; Nuber, B. *Inorg. Chem.* **1996**, *35*, 3936.

(23) (a) Clarke, E. T.; Martell, A. E. *Inorg. Chim. Acta* **1991**, *186*, 103. (b) Motekaitis, R. J.; Sun, Y.; Martell, A. E. *Inorg. Chim. Acta* **1992**, *198−200*, 421.

(24) Flassbeck, C.; Wieghardt, K. *Z. Anorg. Allg. Chem.* **1992**, *608*, 60.

Scheme 2

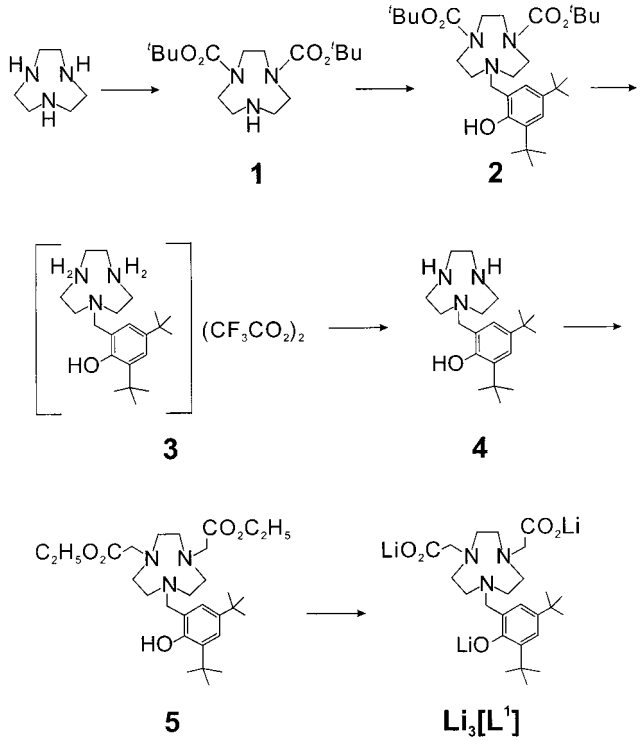

Scheme 3

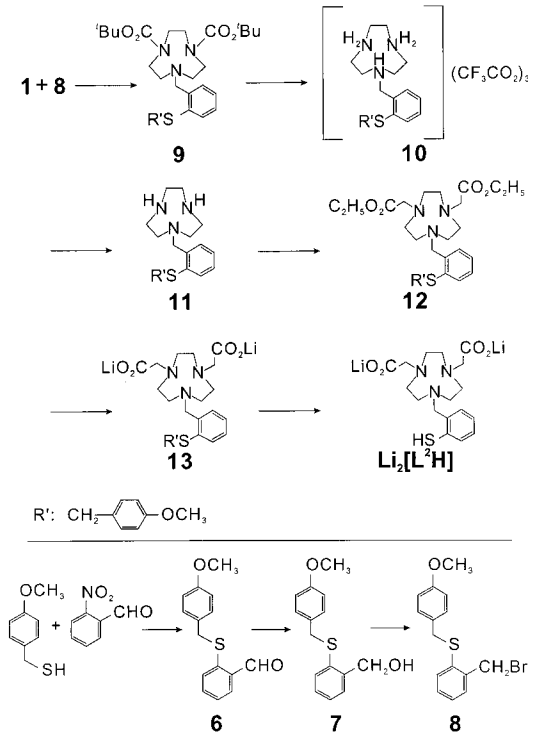

Scheme 4

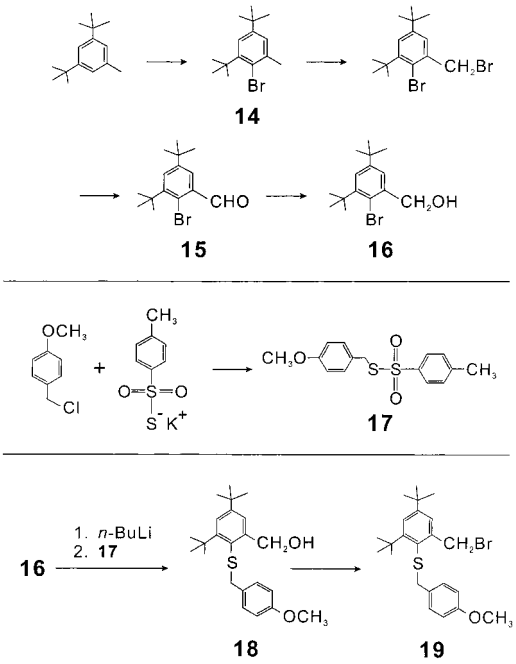

nolate pendent arm. The preparation of such mixed ligands in good yields and high purity is not straightforward.[25]

We have successfully employed a synthetic route where only *two* amine nitrogens of the 1,4,7-triazacyclononane starting material are *N*-protected by its reaction with 2 equiv of 2-*tert*-butoxycarbonyloxyimino-2-phenylacetonitrile (BOC-ON) yielding 1,4,7-triazacyclononane-1,4-dicarboxylic acid di-*tert*-butyl ester (**1**) in 74% yield and high purity (Scheme 2).[26] Compound **1** possesses only one (unprotected) secondary amine to which the desired phenolate or thiophenolate arm can now be appended by the reaction of **1** with either 2-bromomethyl-4,6-di-*tert*-butylphenol (Scheme 2), or 1-bromomethyl-2-(4-methoxybenzylsulfonyl)benzene (**8**, Scheme 3), or 1-bromomethyl-3,5-di-*tert*-butyl-2-(4-methoxybenzylsulfonyl)benzene (**19**, Scheme 4), yielding compounds **2**, **9**, **20**, respectively, which were *N*-deprotected with CF_3COOH in CH_2Cl_2 to give the ammonium salts **3**, **10**, and **21**. Neutralization of these species with base (NaOH or NEt_3) gave the *N*-monosubstituted 1,4,7-triazacyclononane derivatives **4**, **11**, and **22**. The reaction of these compounds with bromoacetic acid ethyl ester produced compounds **5**, **12**, and the precursor of **23** (not isolated) which were deesterified with $LiOH{\cdot}H_2O$, yielding the lithium salt $Li_3[L^1]$ (Scheme 2), **13** (Scheme 3), and **23** (Scheme 5). The S-protected compounds **13** and **23** react with $Hg(acetate)_2$, yielding $Li_2[L^2H]$ and $Li_2[L^3H]$ in good yields (see below).

The synthesis of the sulfenylating agents **8** and **19** for the generation of the S-protected 1,4,7-triazacyclononane derivatives **9** and **20** is outlined in Schemes 3 and 4, respectively. We have successfully used a route described by Shibata et al.[27] who reported the excellent sulfenylating ability of toluene-4-thiosulfonic acid *S*-(4-methoxybenzyl)ester **17**. Thus, in situ lithiated **16** reacts with **17** cleanly to give **18** which reacted with PBr_3 to give **19**. On the other hand, the precursor **8** was synthesized as is shown in Scheme 3 where **6** was generated from 2-nitrobenzaldehyde and (4-methoxyphenyl)methanethiol in DMF. The 4-methoxybenzyl S-protecting group was readily cleaved off from **13** and **23** by $Hg(acetate)_2$ in methanol and passing of H_2S through the solution to produce HgS and the ligands $Li_2[L^2H]$ and $Li_2[L^3H]$, respectively.

The gallium complexes $[Ga^{III}L^1]$, $[Ga^{III}L^2]$, and $[Ga^{III}L^3]$ were prepared in acetonitrile or methanol solutions of $GaCl_3$, the

(25) (a) Erhardt, J. M.; Grover, E. R.; Wuest, J. D. *J. Am. Chem. Soc.* **1980**, *102*, 6365. (b) Weisman, G. R.; Vachon, D. J.; Johnson, V. B.; Gronbeck, D. A. *J. Chem. Soc., Chem. Commun.* **1987**, 886. (c) Blake, A. J.; Fallis, I. A.; Gould, R. O.; Parsons, S.; Ross, S. A.; Schröder, M. *J. Chem. Soc., Chem. Commun.* **1994**, 2467. (d) Wainwright, K. P. *Coord. Chem. Rev.* **1997**, *166*, 35.

(26) (a) Itoh, M.; Hagiwara, D.; Kamiza, T. *Tetrahedron Lett.* **1975**, *16*, 4393. (b) Kovacs, Z.; Sherry, A. D. *Tetrahedron Lett.* **1995**, *36*, 9269.

(27) Shibata, N.; Baldwin, J. E.; Jacobs, A.; Wood, M. E. *Synlett* **1996**, 519.

Scheme 5

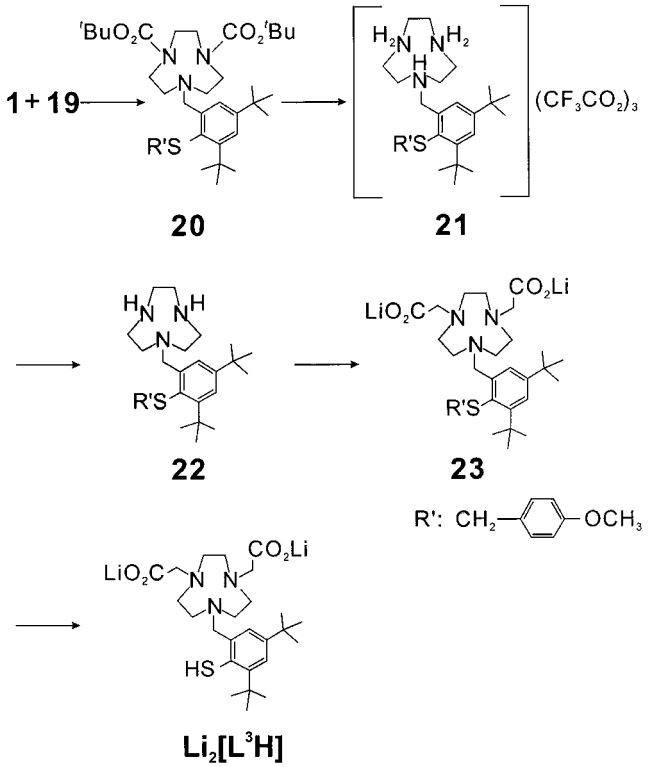

lithium salts of the respective ligand and triethylamine as colorless microcrystalline materials. The corresponding cobalt complexes $[Co^{III}L^1]$, $[Co^{III}L^2]$, and $[Co^{III}L^3]$ were synthesized similarly from $Co^{II}Cl_2 \cdot 6H_2O$ in the presence of air. Compound $[Fe^{III}L^1]$ and $[Fe^{III}L^2]$ were obtained from acetonitrile solutions of $FeCl_3$ and the respective ligand (1:1). All diamagnetic complexes of Ga^{III} and Co^{III} were characterized by ^1H NMR and electro spray ionization (ESI) mass spectrometry (see Experimental Section). From Mössbauer spectroscopy (see below) it was established that the iron complexes $[FeL^1]$ and $[FeL^2]$ both contain a high-spin iron(III) ion. The compound $[FeL^3]$ has not been obtained.

The crystal structures of $[Co^{III}L^1] \cdot CH_3OH \cdot 1.5H_2O$, $[Co^{III}L^3]$, $[FeL^1] \cdot H_2O$, and $[FeL^2]$ have been determined by single-crystal X-ray crystallography at 100 K. Figure 1 shows the structures of the neutral molecules in crystals of the former two, whereas Figure 2 displays the structures of the latter two. Clearly, all species contain a hexadentate macrocyclic ligand with a common 1,4,7-triazacyclononane-1,4-dicarboxylato fragment and an O-, or S-coordinated phenolato or thiophenolato pendent arm.

Table 2 summarizes bond lengths and angles. Structures of complexes containing tris(acetato)-,[20] tris(phenolato)-,[21] and tris(thiophenolato)[22] analogues $[L^a]^{3-}$, $[L^b]^{3-}$, and $[L^c]^{3-}$ (Scheme 1) have been described previously.

Electro- and Spectroelectrochemistry. Cyclic voltammograms (cv) of complexes have been recorded in acetonitrile or dichloromethane solutions containing 0.1 M $[TBA]PF_6$ as supporting electrolyte at 25, −20, −30, or −60 °C. Ferrocene was used as internal standard, and all potentials are referenced versus the Fc^+/Fc couple. Table 3 summarizes the results.

(a) Gallium Complexes. Complexes $[GaL^1]$, $[GaL^2]$, and $[GaL^3]$ contain a redox-inactive Ga^{III} ion. Therefore, all redox activity observed must be ligand-based. As expected, $[GaL^a]$ is redox-inactive in the potential range 1.2 to −2.0 V,[20] whereas $[GaL^b]$ displays three reversible one-electron-transfer waves at

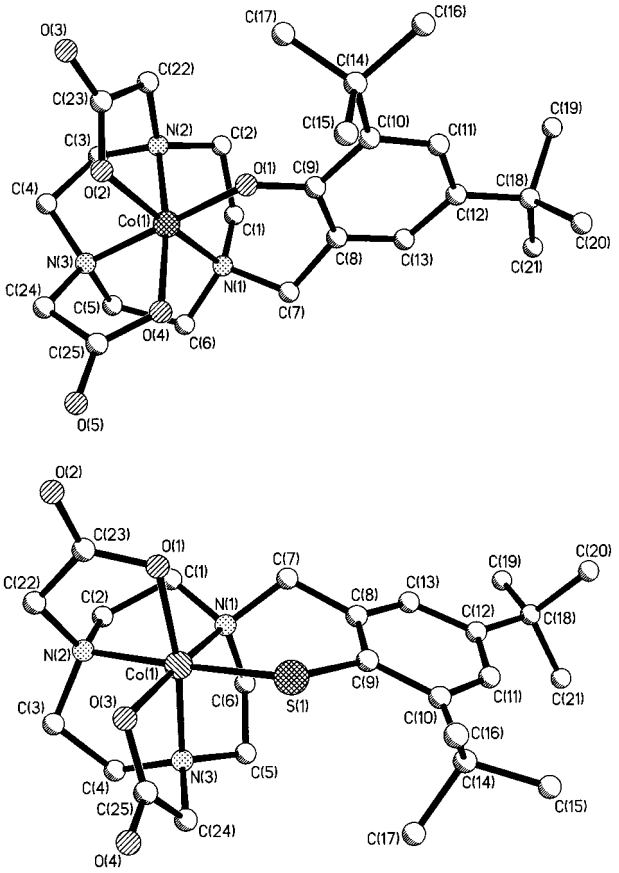

Figure 1. Structures of the neutral molecules in crystals of $[Co^{III}L^1] \cdot CH_3OH \cdot 1.5H_2O$ (top) and $[Co^{III}L^3] \cdot 1.17H_2O$ (bottom).

0.87, 0.62, and 0.35 V which correspond to the reversible formation of one-, two-, and three-coordinated phenoxyl radicals, respectively.[28] In contrast, the tris(thiophenolato) analogue $[GaL^c]$ displays in chloroform only an irreversible, ligand-based oxidation at 1.08 V, which has not been further characterized.[22b]

Figure 3 (top) displays the cv of $[GaL^1]$ which exhibits a single, fully reversible one-electron transfer wave at 0.63 V, corresponding to the generation of a coordinated phenoxyl radical in $[Ga^{III}L^{1\bullet}]^+$. This monocation is stable in solution at ambient temperature. It is paramagnetic with an $S = {}^1/_2$ ground state. The X-band EPR spectrum of the electrochemically generated monocation exhibits a broad, unresolved, isotropic signal at $g = 2.006$ at 50 K (not shown). The electronic spectra of $[GaL^1]$ and its one-electron oxidized form are shown in Figure 4 (top). $[GaL^1]$ is colorless, and the monocation is yellow. The intense absorption maxima at 417 nm ($\epsilon = 4.6 \times 10^3\ M^{-1}\ cm^{-1}$) and 401 nm ($3.9 \times 10^3\ M^{-1}\ cm^{-1}$, sh) are indicative of the phenoxyl radical[28] in $[GaL^{1\bullet}]^+$.

Figure 5 shows the cv's of $[GaL^2]$ and $[GaL^3]$ which were recorded at 25 and −20 °C, respectively (no difference observed). Both species display an irreversible oxidation wave at 0.90 and 0.82 V, respectively, which in the case of $[GaL^2]$ is accompanied by a weak irreversible reduction wave at ∼1.55 V. The latter is only observed if the oxidation wave is scanned first. This indicates that this reduction wave belongs to a species formed after one-electron oxidation has occurred.

This irreversible one-electron oxidation of $[GaL^3]$ has been followed spectroelectrochemically. Three isosbestic points are observed at 279, 250, and 232 nm, and no absorption >380

(28) Adam, B.; Bill, E.; Bothe, E.; Goerdt, B.; Haselhorst, G.; Hildenbrand, K.; Sokolowski, A.; Steenken, S.; Weyhermüller, T.; Wieghardt, K. *Chem. Eur. J.* **1997**, *3*, 308.

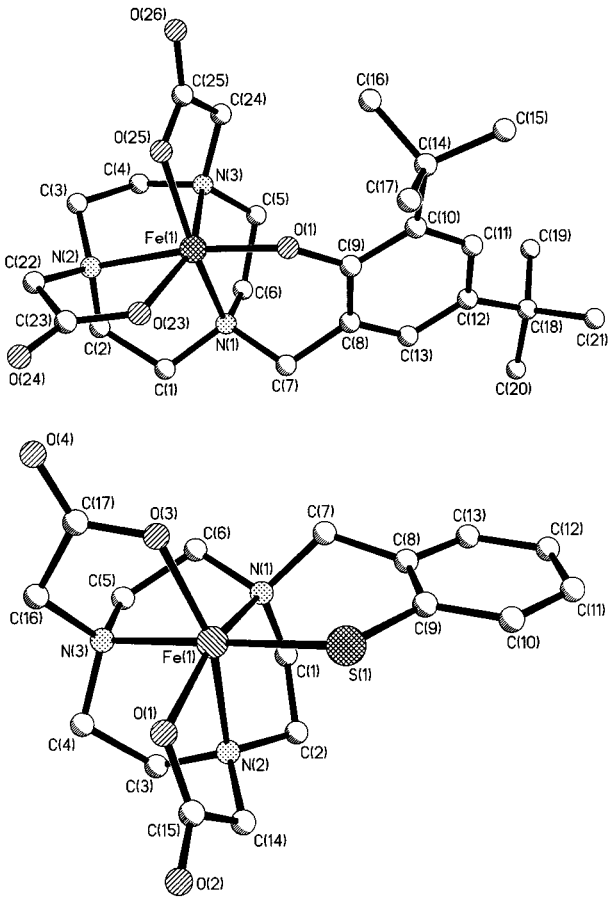

Figure 2. Structures of the neutral molecules in crystals of $[Fe^{III}L^1]\cdot H_2O$ (top) and $[Fe^{III}L^2]$ (bottom).

Table 2. Selected Bond Lengths (Å) of Complexes

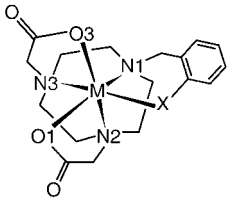

	$[Fe^{III}L^1]\cdot H_2O$[a]	$[Co^{III}L^1]\cdot CH_3OH\cdot 1.5\ H_2O$	$[Fe^{III}L^2]$	$[Co^{III}L^3]\cdot 1.17\ H_2O$
M−X	1.875(4)	1.910(2)	2.3221(4)	2.273(4)
M−O1	1.986(4)	1.918(2)	1.978(1)	1.934(8)
M−O3	1.977(4)	1.937(2)	1.965(1)	1.927(8)
M−N1	2.177(5)	1.928(3)	2.177(1)	1.931(11)
M−N2	2.228(5)	1.928(2)	2.211(1)	1.939(10)
M−N3	2.207(5)	1.951(2)	2.205(1)	1.981(10)

[a] There are four crystallographically independent molecules in the unit cell; the bond lengths of only one molecule are given here.

nm is generated upon oxidation which, as we will show below, immediately rules out the formation of the expected thiyl radical as a stable species. Instead, we propose that the putative $[GaL^{3\bullet}]^+$ radical dissociates rapidly at the Ga−ṠR bond and forms a dangling, uncoordinated thiyl radical which dimerizes rapidly to the disulfide dinuclear complex, $[GaL^3{-}L^3Ga]^{2+}$, shown in Scheme 6. Exactly the same behavior is proposed for $[GaL^2]$ upon oxidation.

(b) Iron Complexes. Figure 3 (middle) shows the cv of $[Fe^{III}L^1]$ which exhibits a reversible oxidative and a reductive one-electron transfer wave at 0.73 V and −1.14 V, respectively. The oxidation is ligand-based and corresponds to the formation

Table 3. Redox Potentials of Complexes[a,b]

complex	*E*, V vs Fc^+/Fc[a]	
$[GaL^1]$	0.63 r.	
$[FeL^1]$	0.73 r.	−1.14 r.
$[CoL^1]$	0.36 r.	−1.38 irr; −0.40 irr.
$[GaL^2]$	0.90 irr.	−1.5 to −1.6 irr.
$[FeL^2]$	0.65 irr.	−0.83 r.
$[CoL^2]$	0.60 irr.	−1.28 irr.
$[GaL^3]$[c]	0.82 irr.	
$[CoL^3]$[c]	0.55 r.	−1.6 irr., −0.5 irr.

[a] For reversible (r.) one-electron processes $E_{1/2}$ is given ($E_{1/2} = (E_{p,ox} + E_{p,red})/2$, whereas for irreversible (irr.) processes the peak potentials $E_{p,ox}$ and/or $E_{p,red}$ are given. [b] Conditions: glassy carbon working electrode, scan rate 100 mV s^{-1}; acetonitrile 0.1 M $[TBA]PF_6$ supporting electrolyte, 25 °C. [c] CH_2Cl_2 solution (0.1 M $[TBA]PF_6$) at −20 °C.

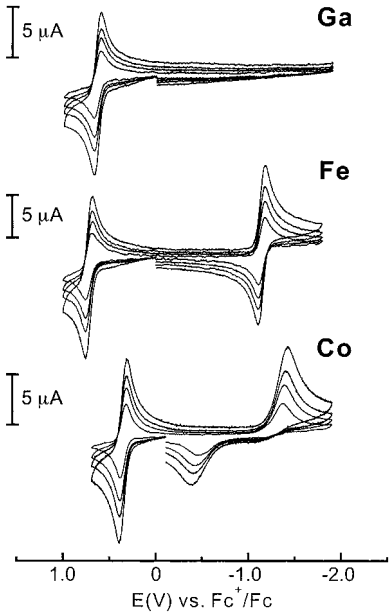

Figure 3. Cyclic voltammograms of $[ML^1]$ complexes (M = Ga, Fe, Co) in CH_3CN solution (0.10 M $[TBA]PF_6$) recorded at scan rates 100, 200, 300, and 500 mV s^{-1} at a glassy carbon electrode at 25 °C.

of a monocationic coordinated phenoxyl radical species $[Fe^{III}L^{1\bullet}]^+$, whereas the reduction is metal-centered, yielding $[Fe^{II}L^1]^-$. The radical cation has been characterized by its absorption spectrum (Figure 4) and its X-band EPR spectrum which is shown in Figure 6. The electronic spectrum of $[Fe^{III}L^1]$ is dominated by an intense phenolato-to-iron charge-transfer band at 520 nm and an absorption minimum at ∼400 nm. The monocation displays the typical intense phenoxyl radical bands at 412, 458, and 523 nm.[28,29]

The X-band EPR spectrum of $[Fe^{III}L^1]$ recorded in perpendicular (normal) mode at 8 K displays a rhombic spectrum with an intense signal at $g \approx 4.3$ typical of an octahedral high-spin iron(III) ion. This signal disappears upon one-electron oxidation, and a relative intense signal at $g \approx 8.5$ is observed in parallel mode at 10 K. This is attributable to $|\Delta M_S| = 2$ transition of an integer spin system ($S = 2$). As shown previously, coordinated phenoxyl radicals ($S_{rad} = {}^1/_2$) couple strongly in an antiferromagnetic fashion to a high-spin iron(III) ion ($S_{Fe} = {}^5/_2$), yielding the observed $S_t = 2$ ground state.[28,29] We have also measured the Mössbauer spectra of $[Fe^{III}L^1]$ and its one-electron oxidized form $[Fe^{III}L^{1\bullet}]^+$ which are shown in Figure 7. From

(29) Snodin, M. D.; Ould-Moussa, L.; Wallmann, U.; Lecomte, S.; Bachler, V.; Bill, E.; Hummel, H.; Weyhermüller, T.; Hildebrandt, P.; Wieghardt, K. *Chem. Eur. J.* **1999**, *5*, 2554.

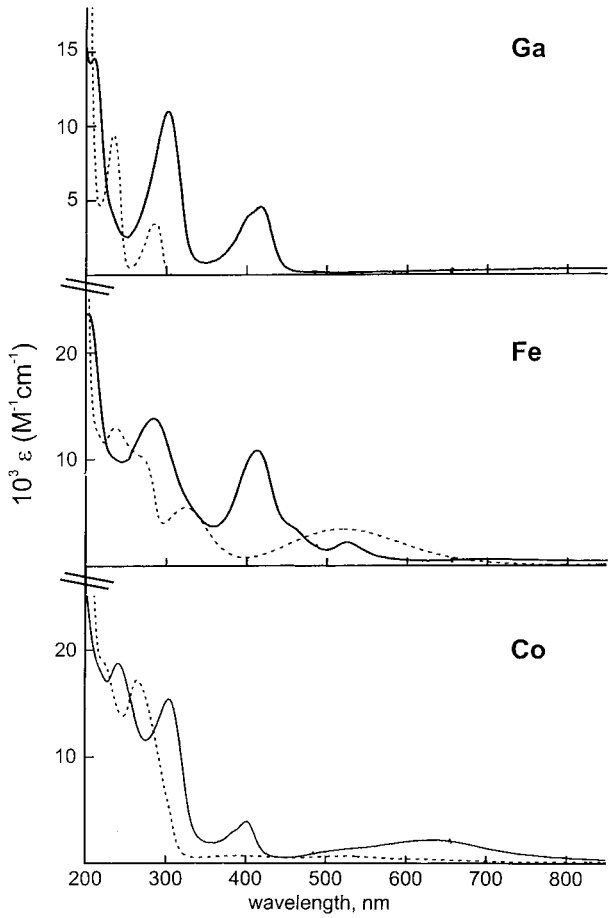

Figure 4. Electronic spectra of $[ML^1]$ (- - -) and $[ML^{1\bullet}]^+$ (—) species in CH_3CN (0.10 M $[TBA]PF_6$); M = Ga, Fe, Co.

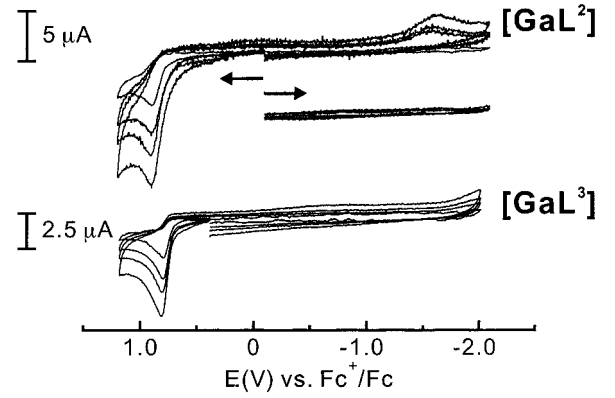

Figure 5. Cyclic voltammograms of $[GaL^2]$ at 25 °C in CH_3CN and $[GaL^3]$ at −20 °C in CH_2Cl_2 solution (0.10 M $[TBA]PF_6$) recorded at scan rates 100, 200, 300, and 500 mV s^{-1} at a glassy carbon electrode.

simulations the following spin Hamiltonian parameters were found: For $[Fe^{III}L^1]$ an isomer shift, δ, of 0.46 mm s^{-1} and quadrupole splitting parameter, $\Delta E_Q = -0.74$ mm s^{-1}, were established at 4.2 K from an applied field (7 T) spectrum ($\eta = 1$; $A_{iso}/g_N\beta_N = -211$ T). These data are typical for octahedral high-spin iron(III) complexes.[28,29] For $[Fe^{III}L^{1\bullet}]^+$ these values do not change much ($\delta = 0.44$ mm s^{-1} and $|\Delta E_Q| = 0.55$ mm s^{-1} (measured at 80 K in zero-field)). This clearly demonstrates that one-electron oxidation of $[Fe^{III}L^1]$ is not metal-centered (no formation of Fe(IV)).

The cv of $[Fe^{III}L^2]$ in acetonitrile (0.10 M $[TBA]PF_6$) at 25 °C (Figure S1) exhibits an irreversible oxidation at $E_{p,ox} = 0.65$ V at a scan rate of 100 mV s^{-1} and a reversible one-electron

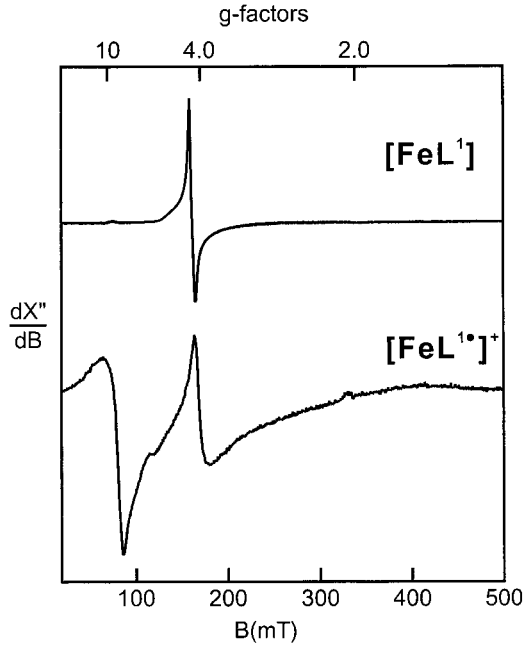

Figure 6. X-band EPR spectra of frozen CH_3CN solution at $[FeL^1]$ at 8 K measured in perpendicular (normal) mode (top) and of $[FeL^{1\bullet}]^+$ in frozen CH_3CN (0.10 M $[TBA]PF_6$) measured in the parallel mode at 10 K. Conditions (top) frequency: 9.6325 GHz; power: 0.1 mW; modulation: 19.9 G; (bottom) frequency: 9.3465 GHz; power: 5.1 mW; modulation: 19.9 G.

Scheme 6

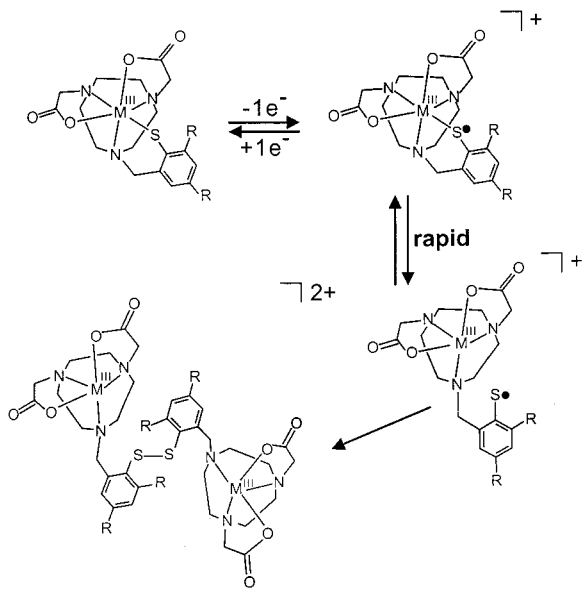

$[M^{III}L^2]$ M=Ga, Fe, Co; R=H

$[M^{III}L^3]$ M=Ga; R=^{t}Bu

reduction at −0.83 V which is assigned to the Fe^{III}/Fe^{II} couple. Thus, the phenolato pendent arm in $[Fe^{III}L^1]$ stabilizes the ferric oxidation state by 310 mV as compared to its thiophenolato analogue $[Fe^{III}L^2]$ but by 840 mV as compared to three-coordinated carboxylates in $[Fe^{III}L^a]$.[20a] The irreversible oxidation wave probably involves the generation of a coordinated thiyl radical which rapidly undergoes $Fe^{III}-\dot{S}R$ bond scission and dimerization, yielding an $[FeL^2-L^2Fe]^{2+}$ disulfide species (Scheme 6). Due to this disulfide formation the cv displays upon re-reduction a small, broad reduction peak at ∼−0.3 V which

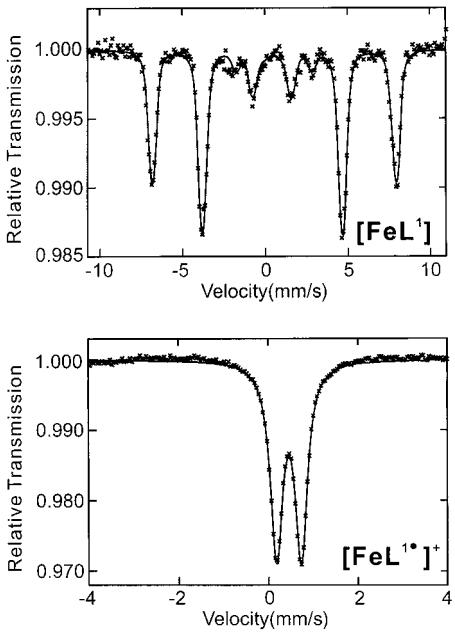

Figure 7. Applied field (7 T) Mössbauer spectrum at 4.2 K of a frozen CH_3CN solution of $[Fe^{III}L^1]$ (top) and simulation (solid line) using spin Hamiltonian parameters given in the text. Bottom: zero-field Mössbauer spectrum at 80 K of a frozen CH_3CN (0.10 M $[TBA]PF_6$) solution of electrochemically generated $[^{57}FeL^{1\bullet}]^+$ (0.5 mM). The isomer shift, δ, is referenced vs α-Fe at 298 K.

is not observed scanning the potential range +0.1 to −2.0 V only.

(c) Cobalt Complexes. The cv of $[Co^{III}L^1]$ shown in Figure 3 displays a reversible one-electron oxidation wave at 0.36 V and a reduction peak at −1.38 V which is accompanied by a reoxidation peak at −0.40 V. Coulometric and spectroelectrochemical measurements at a fixed potential of −1.5 V show that this reduction is a one-electron process which does not lead to decomposition of the reduced form $[Co^{II}L^1]^-$ since subsequent reoxidation quantitatively regenerates the spectrum of $[Co^{III}L^1]$. The irreversible appearance of this process is attributed to slow electrode-to-complex electron-transfer kinetics frequently observed for Co^{III}/Co^{II} couples. Thus, the reduction of $[Co^{III}L^1]$ is metal-centered.

In contrast, the one-electron oxidation is ligand-based. A coordinated phenoxyl radical, $[Co^{III}L^{1\bullet}]^+$, is generated as was judged by its electronic spectrum shown in Figure 4.[30] An intense new maximum at 402 nm ($\epsilon = 3.8 \times 10^3$) and maxima at 634 ($2.1 \times 10^3$), 532 ($1.3 \times 10^3$, sh) indicate the phenoxyl radical formation. The X-band EPR spectrum of $[Co^{III}L^{1\bullet}]^+$ in frozen acetonitrile at 90 K shown in Figure 8 displays a broad, nearly isotopic signal which was simulated with parameters $g_x = 2.0076$, $g_y = 2.0095$, $g_z = 2.0044$ and hyperfine coupling of the organic radical to the ^{59}Co ($I = {}^7/_2$) nucleus of $A^{Co}{}_{xx} = A^{Co}{}_{yy} = 2.2$ G, $A_{zz} = 13.6$ G ($A^{Co}{}_{iso} = 6.0$ G). The hyperfine splitting is not resolved. These parameters are very similar to those reported for $[Co^{III}(L^{Pr\bullet})(acac)]^{2+}$ where HL^{Pr} is 1,4-diisopropyl-7-(3,5-di-*tert*-butyl-2-hydroxybenzyl)-1,4,7-triazacyclononane and $acac^-$ is pentane-2,4-dionate ($g = 2.0047$; $A^{Co}{}_{iso} = 6.0$ G, $a^{H}{}_{iso} = 6.55$ G).[30] In this case the hyperfine splitting was clearly resolved.

In contrast, the cv of $[Co^{III}L^2]$ in acetonitrile (not shown) displays an irreversible one-electron oxidation peak at 0.60 V

(30) Sokolowski, A.; Adam, B.; Weyhermüller, T.; Kikuchi, A.; Hildenbrand, K.; Schnepf, R.; Hildebrandt, P.; Bill, E.; Wieghardt, K. *Inorg. Chem.* **1997**, *36*, 3702.

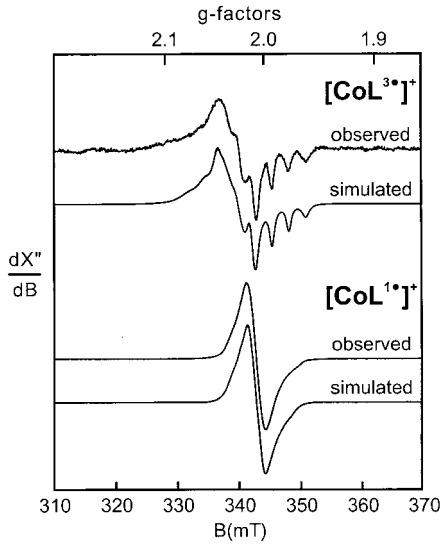

Figure 8. X-band EPR spectra of electrochemically generated (−60 °C) $[Co^{III}L^{3\bullet}]^+$ (top) at 90 K in frozen CH_2Cl_2 (0.10 M $[TBA]PF_6$) and of $[Co^{III}L^{1\bullet}]^+$ (bottom) in CH_3CN (0.10 M $[TBA]PF_6$) solution at 90 K, respectively. Conditions (top and bottom): frequency: 9.6366, 9.6345 GHz; power: 4.0 and 0.1 mW; modulation: 5.7 and 5.7 G.

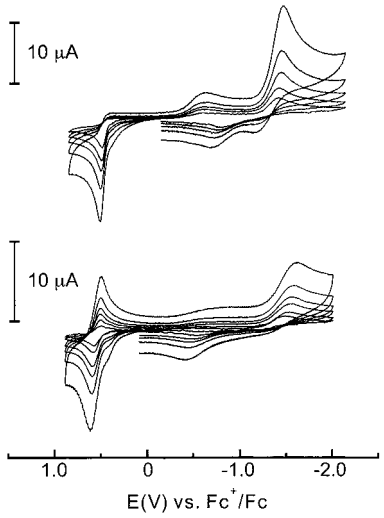

Figure 9. Cyclic voltammograms of $[Co^{III}L^3]$ in CH_3CN (0.10 M $[TBA]PF_6$) at 25 °C at scan rates 100, 200, 300, 500, and 1000 mV s^{-1} (top) and in CH_2Cl_2 (0.10 M $[TBA]PF_6$) at −20 °C at scan rates 50, 100, 200, 300, 500, and 1000 mV s^{-1} (bottom).

which is independent of the scan rate (50−500 mV s^{-1}) and an irreversible reduction peak at −1.28 V which probably corresponds to the metal-centered but kinetically hindered Co^{III}/Co^{II} couple. We have not investigated the electrochemistry of this species in further detail.

The electrochemistry of $[Co^{III}L^3]$ is interesting. The cv of $[CoL^3]$ in acetonitrile at 25 °C shown in Figure 9 (top) displays an irreversible oxidation at $E_{p,ox} = 0.53$ V which is nearly independent of the scan rate (100−1000 mV s^{-1}) and an irreversible reduction at $E_{p,red} = -1.36$ V which is more clearly dependent on the scan rate. The latter is again assigned to the Co^{III}/Co^{II} couple, whereas the former involves the oxidation of the coordinated thiophenolate. Under these experimental conditions the thiyl radical dissociates via Co−ṠR bond scission and dimerizes with formation of a disulfide $[Co^{III}L^3{-}L^3Co^{III}]^{2+}$ as described above for $[GaL^3]$. After scanning through the oxidation wave upon re-reduction, a small wave at −0.5 V is observed. This peak is not observed when the reduction scan is

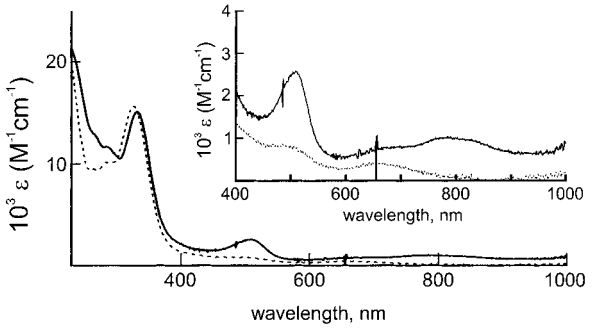

Figure 10. Electronic spectra of [CoL^3] (- - -) and electrochemically generated [$Co^{III}L^{3\bullet}]^+$ (—) at −61 °C in CH_2Cl_2 (0.10 M [TBA]PF_6). The latter spectrum was obtained as described in the text from solutions of [CoL^3] (1 mM) which were oxidized to 30 and 50% only.

started at 0 V. It probably corresponds to the reduction of the putative disulfide complex.

Figure 9 (bottom) displays the cv of [$Co^{III}L^3$] recorded in dichloromethane (0.1 M [TBA]PF_6) at −20 °C at scan rates 50−1000 mV s^{-1}. A reversible one-electron transfer wave is now observed at 0.55 V; $\Delta E_p = E_{p,ox} - E_{p,red} = 80$ mV at scan rates >200 mV s^{-1}. In addition, a kinetically delayed reduction peak at −1.6 V and a corresponding oxidation peak at −0.5 V are observed which are assigned to the Co^{III}/Co^{II} couple. The cv recorded at 25 °C shows the same behavior, but the oxidation wave is only quasi-reversible.

We have investigated the one-electron oxidation of [$Co^{III}L^3$] in CH_2Cl_2 solution, yielding [$Co^{III}L^{3\bullet}]^+$ by spectroelectrochemistry and coulometry. Figure 10 shows the electronic spectra of the starting material [$Co^{III}L^3$] and of its one-electron oxidized form [$Co^{III}L^{3\bullet}]^+$ in CH_2Cl_2 at −61 °C. The latter spectrum has been calculated in the following manner. A solution of [$Co^{III}L^3$] in CH_2Cl_2 (1 mM) has been oxidized at a fixed potential of +0.7 V by controlled potential coulometry to only 30 and 50% with respect to the starting material. The resulting electronic spectra were recorded, and contributions from unreacted starting material were subtracted. The resulting spectra for [$Co^{III}L^{3\bullet}]^+$ were identical in both cases, indicating the stability of both species on the time scale of these experiments (1−2 min) using the above experimental conditions at −61 °C.

The electronic spectrum of [$Co^{III}L^3$] exhibits two relatively weak d−d transitions in the visible at 659 nm (ϵ = 430 M^{-1} cm^{-1}) and 485 nm (870 M^{-1} cm^{-1}). Upon one-electron oxidation the spectrum changes significantly. Intense new, asymmetric maxima appear at 509 nm ($\epsilon = 2.6 \times 10^3$ M^{-1} cm^{-1}) and 784 nm (1.03×10^3 M^{-1} cm^{-1}) with a shoulder at 670 nm. These spectral features resemble closely those reported for the phenylthiyl radical[7] which displays a broad, asymmetric maximum at 460 nm ($\epsilon = 2.5 \times 10^3$ M^{-1} cm^{-1}). Reports on the spectrum of this radical in the literature encompass only an experimental range <550 nm, and no information is available on longer wavelength maxima. The spectra of [$Co^{III}L^{1\bullet}]^+$ (Figure 4) and [$Co^{III}L^{3\bullet}]^+$ (Figure 10) are rather similar. This points to the formation of a moderately stable thiyl radical in [$Co^{III}L^{3\bullet}]^+$.

That this thiyl radical is coordinated to a cobalt(III) ion in [$Co^{III}L^{3\bullet}]^+$ was unambiguously proven by X-band EPR spectroscopy. Figure 9 (top) shows this spectrum of a frozen CH_2Cl_2 (0.1 M [TBA]PF_6) solution of [$Co^{III}L^{3\bullet}]^+$ at 90 K. The electrochemical generation of the radicals was performed at −60 °C, and care was taken to ensure that the samples never warmed up before or during the recording of this EPR spectrum.

The EPR spectrum exhibits a rhombic signal at $g \approx 2$ and well-resolved hyperfine splitting between an organic radical spin $S = {}^1/_2$ and the ^{59}Co nucleus ($I = {}^7/_2$). The spectrum was successfully simulated by using the following parameters: $g_x = 2.0339$, $g_y = 2.0159$, $g_z = 2.0180$, $A_{xx}(^{59}Co) = 2.2$ G; $A_{yy}(^{59}Co) = 2.5$ G; $A_{zz}(^{59}Co) = 27.3$ G; $A_{iso}(^{59}Co) = {}^1/_3(A_{xx} + A_{yy} + A_{zz}) = 10.7$ G, $g_{iso} = 2.0226$.

In comparison, the 2,4,6-tri-*tert*-butylphenylthiyl radical generated in the solid state by photolysis shows an axial spectrum with $g_\perp = 2.015$ and $g_{\times e7 \times e7} = 2.003$.[10,31d] EPR studies of Jeevarajan, Fessenden, and others show that the Ph-S$^\bullet$ radical has a high g factor of 2.0252, indicating that the unpaired spin is highly localized on the sulfur[31] (no hyperfine splitting to the phenyl protons has been reported).

Mass Spectroscopic Evidence for Dimer Formation. To obtain evidence for the dimer formation during the electrochemical oxidations of [CoL^3], [GaL^2], and [GaL^3] we have chemically oxidized these species in CH_3CN solutions at −35 °C and recorded their electrospray mass spectra. As reagents we have used the outer-sphere one-electron oxidants [$Ni^{III}(tacn)_2$]-$(ClO_4)_3$ (for [CoL^3]) (tacn = 1,4,7-triazacyclononane) and the thianthrene radical monocation tetrafluoroborate (for [GaL^2] and [GaL^3]) in 10−20% excess.

Immediately after completion of these chemical oxidations the ESI mass spectra were recorded. For [CoL^3] an $m/z = 1169.6$ peak corresponds to $\{[CoL^3-L^3Co](ClO_4)\}^+$. Similarly, for [$GaL^2$] the $m/z = 885.2$ peak corresponds to $\{[GaL^2-L^2Ga]F\}^+$, and for GaL^3 the peak $m/z = 1109.4$ corresponds to the monocation $\{[GaL^3-L^3Ga]F\}^+$. In addition strong peaks m/z, where $z = 2$, have been observed at 535.2 for the dinuclear dication of oxidized [CoL^3]; at 433.2 and 434.0 two peaks corresponding to a ^{69}Ga:^{71}Ga ratio of 60:40 for the dinuclear dication $[GaL^2-L^2Ga]^{2+}$ have been observed. The observation of the latter m/z peaks rules out the possibility that the m/z with $z = 1$ peaks correspond to monocationic clusters consisting only of two mononuclear cations [$ML^{\bullet}]^+$ and an anion.

Discussion

In the following section we will first focus on the thermodynamic and spectroscopic features of phenylthiyl radicals—uncoordinated and coordinated to a metal ion.

The redox potentials relative to the standard hydrogen electrode (SHE) for the uncoordinated species [*p*-X-C_6H_4-$Y^{\bullet}$]/[*p*-X-C_6H_4-$Y]^-$ and [*p*-X-C_6H_4-$Y^{\bullet}H]^+$/[*p*-X-C_6H_4-YH] (where X represents H or a methyl group and Y is either oxygen or sulfur) have been measured in aqueous solution by pulse radiolytic studies of electron-transfer equilibria.[32] To compare these values to those obtained in the present study by cyclic voltammetry we have subtracted 0.40 V from the values referenced versus SHE[32] since the Fc^+/Fc couple has a redox potential of 0.400 V versus SHE.[33] We have also assumed that the measured peak potentials, $E_{p,ox}$, for the irreversible one-electron oxidations of [ML] complexes in Table 3 are related to the unknown half-wave potentials, $E_{1/2}$, by the equations $E_{1/2} = (E_{p,ox} + E_{p,red})/2$ and $\Delta E = (E_{p,ox} - E_{p,red}) = 80$ mV at a 100 mV s^{-1} scan rate under our experimental conditions. These $E_{1/2}$ values are ordered in a redox potential ladder in Figure 11.

From columns 1−4 the following conclusions can be drawn which all reflect the fact that thiyl radicals are S-centered,

(31) (a) Cited in ref 7. (b) Jeevarajan, A. S.; Fessenden, R. W. *J. Phys. Chem.* **1992**, *96*, 1520. (c) Schmidt, U.; Müller, A. *Angew. Chem.* **1963**, *75*, 299; *Angew. Chem., Int. Ed. Engl.* **1963**, *2*, 216. (d) Rundel, W.; Scheffler, K. *Z. Naturforsch.* **1963**, *18b*, 984.

(32) Armstrong, D. A.; Sun, Q.; Schuler, R. H. *J. Phys. Chem.* **1996**, *100*, 9892.

(33) (a) Koepp, H. M.; Wendt, H.; Strehlow, H. *Z. Elektrochem.* **1960**, *64*, 483. (b) Gagné, R. R.; Koval, C. A.; Lisensky, G. C. *Inorg. Chem.* **1980**, *19*, 2854.

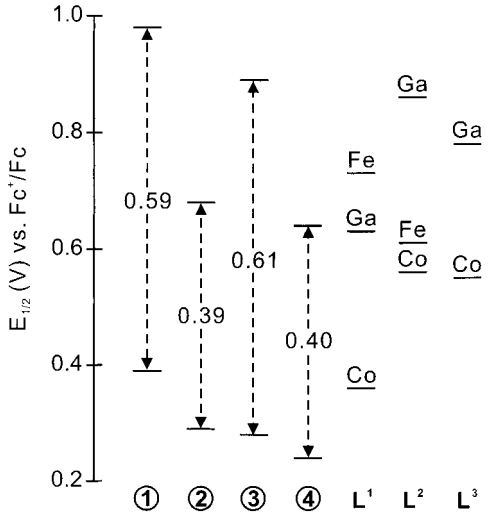

Figure 11. Redox potential ladder for phenoxyl and phenylthiyl (coordinated and uncoordinated) radicals. Potentials are referenced vs the Fc^+/Fc couple where the potentials given in columns 1, 2, 3, and 4 have been obtained by subtracting 0.40 V from the values given in ref 32 vs NHE. Columns L^1, L^2, L^3 give the redox potentials for the couples $[ML^{\bullet}]^+/[ML]$ from the present work where the $E_{p,ox}$ values for irreversible processes given in Table 3 were converted to $E_{1/2}$ values by subtracting 40 mV, assuming that $E_{1/2} = (E_{p,ox} + E_{p,red})/2$ and $\Delta E = (E_{p,ox} - E_{p,red}) = 80$ mV under our experimental conditions (scan rate 100 mV s^{-1}). Column 1 gives values for the couples $[C_6H_5\dot{O}H]^+/[C_6H_5OH]$ (top value) and $[C_6H_5O^{\bullet}]/[C_6H_5O]^-$ (lower value); column 2, those of the couples $[C_6H_5\dot{S}H]^+/[C_6H_5SH]$ (top) and $[C_6H_5S^{\bullet}]/[C_6H_5S]^-$ (bottom); column 3, those of the corresponding *p*-methylphenol(ate) derivatives; and 4, those of the corresponding *p*-methylthiophenol(ate) derivatives.

contrasting in this respect the phenoxyls which are delocalized:[32] (i) The one-electron oxidation of phenolate or *p*-methylphenolate is energetically more favorable by ~600 mV than the corresponding oxidations of the phenol and *p*-methylphenol (columns 1 and 3). This difference is reduced to ~400 mV for the corresponding thio-derivatives in columns 2 and 4. (ii) As expected, the substitution of the parent phenol (or thiophenol) at the para position by an electron-donating methyl group lowers the redox potentials for the respective phenolates and phenols by 110 and 90 mV (columns 1, 3), respectively, which decreases to 50 and 40 mV, respectively, for the thio derivatives (columns 2 and 4). (iii) It is always easier to oxidize the analogous thio derivatives than their corresponding oxygen analogues by 50−100 mV (compare columns 1, 2 with 3, 4). Clearly, protonation of a given phenolate or thiophenolate has the most dramatic effect on the respective redox potential.

We now turn to the thermodynamic properties of coordinated phenoxyl and thiyl radicals. In previous work on tris(phenolato)-metal complexes, (M = Ga, Co, Fe), we had established that the redox potentials for the couples $[ML^{c\bullet}]^+/[ML^c]$ vary from 0.35 V for the gallium[28] to 0.38 V for the iron[28] and to 0.01 V for the cobalt complex.[30] It was shown that they correlate with the π donor bond strength of the $M-O_{phenolato}$ bond which is the least strong one in low-spin Co^{III} (t_{2g}^6) complexes, but relatively strong in Ga^{III} (d^0), and the strongest one in high-spin Fe^{III} (d^5) complexes. Exactly the same order of the redox potentials, namely $E_{1/2}$ is the lowest for $[CoL^1]$, intermediate for $[GaL^1]$, and highest for $[FeL^1]$, has been found in the present work. It is therefore rather unexpected that the redox potentials for the $[ML^{2\bullet}]^+/[ML^2]$ couples display a different order. Whereas the potential for the cobalt(III) species, $[CoL^2]$, is still the lowest, it is closely followed by that for $[FeL^2]$, and that for $[GaL^2]$ is significantly higher. For the series $[ML^3]$ this order could not be established, because $[FeL^3]$ is not available, but the potential for $[GaL^3]$ is again very much higher than that observed for $[CoL^3]$. This is an indication that the Ga−S bond is significantly stronger than the Fe−S bond. Both metal ions are expected to display more π acidity due to their empty and half-filled t_{2g} subshell, respectively, contrasting in this respect the filled t_{2g}^6 subshell of a cobalt(III) ion. It is also quite remarkable that oxidation of the coordinated phenolate to the corresponding phenoxyl in $[ML^1]$ complexes is more easily achieved than oxidation of the analogous thiophenolate complexes. This is, as described above, in contrast to the electrochemistry of the uncoordinated ligands in column 1−4. We take this as an experimental indication that the metal-to-sulfur (thiophenolate) bonds possess significantly more covalent character than the metal-to-oxygen (phenolate) bonds.

The electronic spectra of $[CoL^{1\bullet}]^+$, $[GaL^{1\bullet}]^+$, and $[FeL^{1\bullet}]^+$ (Figure 4 and Table 4) clearly show the presence of a phenoxyl radical by their intense ($\epsilon > 3 \times 10^3$ M^{-1} cm^{-1}) asymmetric transitions 380−420 nm and a less intense transition >600 nm. This has been reported for numerous (phenoxyl)metal complexes, irrespective of the nature of the metal ion.[12] It is therefore gratifying that the electronic spectrum of $[Co^{III}L^{3\bullet}]^+$ shows exactly the same features: an intense, broad, and asymmetric transition at 509 nm ($\epsilon = 2.6 \times 10^3$ M^{-1} cm^{-1}) and a transition at 784 nm ($\epsilon = 1.0 \times 10^3$ M^{-1} cm^{-1}). As pointed out above, the former transition resembles closely that reported for the free phenylthiyl radical at 460 nm ($\epsilon = 2.5 \times 10^3$ M^{-1} cm^{-1}).[7,34]

The X-band EPR spectrum of the uncoordinated phenylthiyl radical shows a large *g*-value anisotropy which has been interpreted in terms of spin−orbit coupling ($g_{iso} = 2.0252$),[31] which mixes two states of different orbital angular momentum. In the ground state of the radical the unpaired electron is localized in a nonbonding orbital of the sulfur,[8a,b] and consequently, no resolved hyperfine splitting to the protons of the phenyl ring has been detected. This is in marked contrast to phenoxyl radicals, the EPR spectra of which display typical organic radical signals at $g \approx 2.0045$ with well-resolved hyperfine splitting to phenyl protons due to significant delocalization of the unpaired electron over the phenyl ring.[35]

In Table S21 we have summarized EPR spectroscopic data on cobalt(III) complexes containing coordinated phenoxyl,[30,36] anilino,[37] thiyl, and semiquinonato[38−40] ligands. With the exception of the present (thiyl)cobalt complex, $[Co^{III}L^{3\bullet}]^+$, all complexes display EPR signals centered at $g \approx 2.00$ with, in most cases, well-resolved ^{59}Co hyperfine splitting typical for the presence of a coordinated organic radical. For (semiquinonato)cobalt(III) complexes the $A(^{59}Co)$ hfcs are observed in the rather narrow range 9.8−11 G,[38−40] whereas for (phenoxyl)-cobalt(III) species[30,36] this value is significantly smaller in the range 5−6 G. The semiquinonates are O,O-coordinated bidentate ligands, whereas the phenoxyls are O-coordinated monodentate. It has recently been shown[37] that a monodentate anilino radical coordinated to a cobalt(III) ion displays a rather strong ^{59}Co

(34) Bonifacic, M.; Weiss, J.; Chaudhry, S. A.; Asmus, K.-D. *J. Phys. Chem.* **1985**, *89*, 3910.
(35) (a) Neta, P.; Fessenden, R. W. *J. Phys. Chem.* **1974**, *78*, 523. (b) Stone, T. J.; Waters, W. A. *J. Chem. Soc.* **1964**, 213.
(36) Müller, J.; Kikuchi, A.; Bill, E.; Weyhermüller, T.; Hildebrandt, P.; Ould-Moussa, L.; Wieghardt, K. *Inorg. Chim. Acta* **2000**, *297*, 265.
(37) Penkert, F. N.; Weyhermüller, T.; Bill, E.; Hildebrandt, P.; Lecomte, S.; Wieghardt, K. *J. Am. Chem. Soc.* **2000**, *122*, 9663.
(38) Wicklung, P. A.; Beckmann, L. S.; Brown, D. G. *Inorg. Chem.* **1976**, *15*, 1996.
(39) Buchanan, R. M.; Pierpont, C. G. *J. Am. Chem. Soc.* **1980**, *102*, 4951.
(40) Kessel, S. L.; Emberson, R. M.; Debrunner, P. G.; Hendrickson, D. N. *Inorg. Chem.* **1980**, *19*, 1170.

Table 4. Electronic Spectra of Complexes in CH_3CN Solution

complex	λ_{max}, nm (ϵ, M^{-1} cm^{-1})
$[GaL^1]$	233 (9400), 286 (3500)
$[GaL^{1\bullet}]^{+\,a}$	417 (4600), 401 (3900, sh), 302 (1.1×10^4)
$[FeL^1]$	520 (3400), 323 (5400), 272 (9.9×10^3, sh), 236 (1.3×10^4)
$[FeL^{1\bullet}]^{+\,a}$	523 (2100), 458 (3500, sh), 412 (1.1×10^4), 283 (1.4×10^4)
$[CoL^1]$	607 (300, sh), 522 (600), 390 (600), 266 (1.7×10^4), 225 (1.9×10^4, sh)
$[CoL^{1\bullet}]^{+\,a}$	634 (2100), 532 (1300, sh), 402 (3800), 304 (1.5×10^4), 241 (1.9×10^4)
$[GaL^2]$	292 (1.6×10^3, sh), 262 (1.3×10^4, sh)
$[FeL^2]$	595 (2800), 450 (900,sh), 291 (9600), 253 (1.3×10^4)
$[CoL^2]$	629 (300), 504 (500,sh), 402 (1.1×10^3), 311 (1.7×10^4), 230 (1.9×10^4, sh)
$[GaL^3]$	283 (2000, sh), 252 (1.3×10^4)
$[CoL^3]$	639 (520), 489 (1.0×10^3), 322 (1.9×10^4), 281 (1.2×10^4, sh), 224 (2.5×10^4, sh)
$[CoL^3]^{\,b}$	659 (430), 485 (870), 326 (1.6×10^4), 286 (1.0×10^4), 262 (9.6×10^3)
$[CoL^{3\bullet}]^{+\,a,b}$	784 (1.0×10^3), 670 (790, sh), 509 (2600), 332 (1.5×10^4), 284 (1.2×10^4), 267(1.3×10^4, sh)

[a] Electrochemically generated (0.10 $[TBA]PF_6$). [b] CH_2Cl_2 solution.

hyperfine coupling of 12.15 G (in addition to strong nitrogen hyperfine coupling and coupling to the N−H proton). The observed EPR spectrum of $[CoL^{3\bullet}]^+$ is fully in line with the interpretation as a cobalt(III) species containing a coordinated thiyl radical: a high g_{iso} value of 2.0226 and the absence of phenyl proton hyperfine coupling indicates its S-centered character. Interestingly, the ^{59}Co hyperfine coupling of 10.7 G is rather large. We take this as an indication that the Co−S bond in $[Co^{III}L^{3\bullet}]^+$ is strong and covalent as is the Co−N bond in the anilino radical species $[Co^{III}(L^{NH\bullet})(Bu_2acac)]^{2+}$ where $(L^{NH})^{1-}$ represents the monoanion of 1-(2-amino-3,5-di-*tert*-butylbenzyl)-4,7-dimethyl-1,4,7-triazacyclononane.[37] The Co−O bond in (phenoxyl)cobalt(III) species is then considerably less covalent.[36,30]

Conclusions

We have shown that the mononuclear, neutral complexes of Ga^{III}, Fe^{III}, Co^{III} containing a trisanionic macrocyclic ligand with one *o*,*p*-substituted phenolate and two carboxylate pendent arms, $[ML^1]$, are reversibly one-electron oxidized, yielding stable (phenoxyl)metal(III) cations $[ML^{1\bullet}]^+$ which were characterized by their electronic EPR and, in case of iron, by their Mössbauer spectra. It is unequivocally shown that in these instances ligand-based oxidations occur rather than metal-based.

Replacing the phenolate pendent arm by an *o*,*p*-di-*tert*-butylthiophenolate in $[L^3]^{3-}$ and the preparation of the complex $[CoL^3]$ has allowed the electrochemical generation of the monocation $[Co^{III}L^{3\bullet}]^+$ in CH_2Cl_2 solution at −61 °C. It has been shown that this species is an S-coordinated phenylthiyl radical which displays characteristic transitions in the visible. The X-band EPR spectrum exhibits a ^{59}Co hyperfine split signal ($A(^{59}Co) = 10.7$ G) at $g_{iso} = 2.0226$. In agreement with the notion that thiyls are S-centered radicals, the above monocation does not show hyperfine splitting to the benzyl or phenyl ring protons.

These coordinated phenylthiyl radicals display significantly enhanced reactivity in solution at 20 °C compared to their phenoxyl analogues. The M−ṠR bonds are quite weak and dissociate in solution with dimerization yielding dinuclear disulfide complexes $[ML{-}LM]^{2+}$.

Ligand abbreviations: $H_3(L^{OCH_3})$ = 1,4-dimethyl-7-(3-*tert*-butyl-5-methoxy-2-hydroxy-benzyl)-1,4,7-triazacyclononane; $L^{Pr}H$ = 1,4-diisopropyl-7-(3,5-di-*tert*-butyl-2-hydroxy-benzyl)-1,4,7-triazacyclononane; Ph_2acac^- = diphenylacetylacetonate; $acac^-$ = 2,4-pentanedionate; Bu_2acac^- = di-*tert*-butylacetylacetonate; $L^{NH}H$ = 1-(2-amino-3,5-di-*tert*-butylbenzyl)-4,7-dimethyl-1,4,7-triazacyclononane; trien = triethylenetetramine; $DBsq^{\bullet-}$ = 3,5-di-*tert*-butyl-*o*-benzosemiquinonate; $DCat^{2-}$ = 3,5-di-*tert*-butylcatecholate; bpy = 2,2′-bipyridine; $salen^{2-}$ = *N*,*N*′-ethylenebis(salicylideneiminate)(2-); Cl_4sq^- = tetrachlorosemiquinonate.

Acknowledgment. We thank the Fonds der Chemischen Industrie and the Deutsche Forschungsgemeinschaft (Priority program "Radicals in Biology") for financial support. Mrs. Heike Schucht is thanked for skillfull help with the X-ray crystallography.

Supporting Information Available: Figure S1 showing the cv of $[Fe^{III}L^2]$; Table S21 summarizes EPR parameters of (radical)cobalt(III) complexes; tables of crystallographic and structure refinement data, atom coordinates, bond lengths and angles, anisotropic thermal parameters, and calculated positional parameters of H atoms (PDF). An X-ray crystallographic file, in CIF format. This material is available free of charge via the Internet at http://pubs.acs.org.

JA004305P